INTERNATIONAL JOURNAL OF HYDROGEN ENERGY XXX (XXXX) XXX

Available online at www.sciencedirect.com

ScienceDirect

journal homepage: www.elsevier.com/locate/he

Review Article

A review on bismuth-based composite oxides for photocatalytic hydrogen generation

Wenjian Fang, Wenfeng Shangguan*

Research Centre for Combustion and Environment Technology, Shanghai Jiao Tong University, Shanghai 200240, PR China

ARTICLE INFO

Article history:
Received 20 August 2018
Received in revised form
5 November 2018
Accepted 8 November 2018
Available online xxx

Keywords:
Photocatalyst
Bismuth-based composite oxides
Water splitting

ABSTRACT

Bismuth-based composite oxides are always considered the best visible-light photocatalysts for oxygen production. However, they are failed to photocatalytic reduce the hydrogen from water, due to their lower conduction band made up by Bi 6p and O 2p. Thus, it is significant to modulate their levels of the conduction and valence bands satisfying the redox potential for both H^+/H_2 and O_2/H_2O, which will directly lead to discovering new visible-light materials for photocatalytic hydrogen generation. Recent years, some modified bismuth-based composite oxides have been reported to achieve photocatalytic hydrogen production. In this paper, a review of photocatalytic hydrogen generation by bismuth-based composite oxides is presented, mainly including energy band engineering, Z-scheme overall water splitting, and strategies for photocatalytic activity improvement.

Contents

Introduction . . . 00
Systems of photocatalytic hydrogen generation . . . 00
History of visible light photocatalytic hydrogen generation . . . 00
Bismuth-based composite oxides for visible light photocatalysis . . . 00
Energy band engineering . . . 00
Doping elements . . . 00
Quantum size effect . . . 00
Solid solution . . . 00
Bi_2O_3 . . . 00
Bi_2WO_6 . . . 00
$BiVO_4$ . . . 00
Others . . . 00
Z-scheme overall water splitting . . . 00
Strategies for photocatalytic hydrogen generation activity improvement . . . 00
Crystal facet engineering . . . 00

* Corresponding author.
E-mail address: shangguan@sjtu.edu.cn (W. Shangguan).
https://doi.org/10.1016/j.ijhydene.2018.11.063
0360-3199/

Please cite this article as: Fang W, Shangguan W, A review on bismuth-based composite oxides for photocatalytic hydrogen generation, International Journal of Hydrogen Energy, https://doi.org/10.1016/j.ijhydene.2018.11.063

Surface modification . . . 00
Effect of different cocatalyst . . . 00
Conclusions . . . 00
Acknowledgment . . . 00
References . . . 00

Introduction

Photocatalytic hydrogen generation from pure water, known as the "holy grail" in chemistry, can convert solar energy directly into green storable chemical energy [1,2].

After decades of development, solar-to-hydrogen energy conversion efficiency has exceeded 1% [3]. However, it is still far from the practical application requirement of at least 10% solar energy conversion efficiency. Thus, photocatalytic hydrogen generation is still in the experimental research stage. Discovering new materials (especially visible-light photocatalysts) and improving solar energy conversion efficiency are still two major themes in research.

Systems of photocatalytic hydrogen generation

There are two main ways for photocatalytic hydrogen production: heterogeneous photocatalytic hydrogen production (HPC) and the photoelectric catalyzed hydrogen production (PEC). Comparision with HPC, PEC is uncompetitive due to its high cost and complex structures. Moreover, HPC can be divided into two styles: photocatalytic hydrogen production with sacrificial agent and overall water splitting. Though photocatalytic hydrogen production with sacrificial agent always achieve high QE, it should be reconsider the consume of sacrificial agent and the stability of photocatalyst. Unless sacrificial agents can be converted to another essential industrial products, we think at present overall water splitting is more meaningful and competitive compared to photocatalytic hydrogen production with sacrificial agent [4].

Overall water spliting is extremely challenging which requires photocatalysts to satisfy the redox potential for both H^+/H_2 (0 V vs NHE) and O_2/H_2O (1.23 V vs. NHE). Additionally, photocatalytic overall water splitting should have two characteristic: stoichiometry of H_2 and O_2 evolution and amounts of H_2 and O_2 evolved steadily with irradiation time. There are two ways to realize overall water splitting under visible light. One is single photocatalyst system which raises harsh requirements for photocatalysts both thermodynamically and kinetically. Another way is to develop two-photon system as photosynthesis [5]. H_2 and O_2 will evolved in different photocatalysts which may be active only for half reactions of water splitting. This Z-scheme is comparatively easier in choosing photocatalysts than single photocatalyst system. On account of the existance of redox mediator, the utilization of photons is decreased in Z-scheme system.

History of visible light photocatalytic hydrogen generation

Since Zou et al. reported the $NiO_x/In_{0.9}Ni_{0.1}TaO_4$ photocatalyst water splitting under visible light irradiation [6], it raised the curtain of exploring new visible-light materials for photocatalytic hydrogen generation. Almost the same time, TiO_2 with a band gap larger than 3.0 eV was modified by several approaches, including the use of dopants, such as N, C, and S, to realize visible-light absorption [7–9]. Among them, TiO_2 through hydrogenation exhibit substantial visible-light-driven photocatalytic hydrogen production with the use of a sacrificial reagent [10]. In 2004, Kudo et al. reported that noble metal ion doped $SrTiO_3$ possess intense absorption bands in the visible light region [11]. Notably, the Rh(1%)-doped $SrTiO_3$ photocatalyst loaded with a Pt cocatalyst (0.1 wt %) can achieve 5.2% of the quantum yield at 420 nm for the H_2 evolution reaction. In 2005, Maeda et al. first found that GaN:ZnO solid solutions with $Rh_{2-x}Cr_xO_3$ co-catalyst can reach 5.9% of quantum yield under visible light irradiation [12–14]. In 2009, Wang et al. discovered metal-free polymeric photocatalyst g-C_3N_4 for hydrogen production from water under visible light [15]. Then carbon nanodot-carbon nitride (Cdot-g-C_3N_4) nanocomposite is demonstrated to split pure water with solar-to-hydrogen energy conversion efficiency exceeding 2% [16]. In 2013, nanocrystalline CoO was proved to be a photocatalyst with a solar-to-hydrogen efficiency of around 5% [17]. Recently, 5.4% energy conversion efficiency at 353 K was achieved by supported black phosphorus nanosheets as hydrogen-evolving photocatalyst [18]. Though both CoO and Co–P photocatalysts show excellent performance, the problem of the stability is unavoidable. Almost simultaneously, Faqrul A. Chowdhury et al. reported that the wafer level photochemical diode consists of vertically aligned InGaN nanosheets could enable relatively efficient overall pure water splitting (STH ~3.3%) [19]. The above is a short history for visible-light photocatalytic hydrogen generation. Additionally, though sulfide such as CdS and ZnCdS have achieved nearly 100% quantum yield at 420 nm [20,21], the photocatalytic hydrogen reaction need the existing of sacrificial agents due to the oxidation of S.

Bismuth-based composite oxides for visible light photocatalysis

Among visible-light photocatalysts, the Bismuth-based composite oxides have received much attention as potential promising photocatalysts for water oxidation since Kudo et al. firstly reported photocatalytic oxygen generation under visible light by Bi_2WO_6 [22] and $BiVO_4$ [23]. As for $BiVO_4$, there are three crystal forms: monoclinic (*m*-$BiVO_4$), tetragonal (z-$BiVO_4$), and tetragonal (t-$BiVO_4$). Among them, *m*-$BiVO_4$ has the best photocatalytic activity. Researchers have devoted much work about $BiVO_4$ to improve photocatalytic activity. Related references have well studied about bismuth-based composite oxides, such as mediating the morphology and structure, constructing heterojunction and doping with different elements [24–36].

Please cite this article as: Fang W, Shangguan W, A review on bismuth-based composite oxides for photocatalytic hydrogen generation, International Journal of Hydrogen Energy, https://doi.org/10.1016/j.ijhydene.2018.11.063

A variety of Bismuth-based composite oxides have been proved as photocatalysts such as Bi_2O_3 [37], Bi_2MO_6(M = Cr, Mo and W) [38–42], $BiMO_4$(M = P, V, Nb and Ta) [43–45], BiOX (X = Cl, Br and I) [46], $BiFeO_3$ [47], $BiYO_3$ [48], $(BiO)_2CO_3$ [49], and pentavalent bismuthates [50–52]. However, Bismuth-based composite oxides are failed to photocatalytic reduce the hydrogen from water, due to their lower conduction band not satisfying the reduction potential of H^+ to H_2 as shown in Fig. 1. Thus, it may be exciting if these bismuth-based composite oxides can also be able to photocatalytic hydrogen generation. If so, more and more new visible-light materials for photocatalytic hydrogen generation would be discovered. Recent years, some modified Bismuth-based composite oxides have been reported to achieve photocatalytic hydrogen production. To modulate their levels of the conduction and valence bands, meeting the potential requirements of reduction and oxidation of H_2O at the same time, is significant. On the other hand, building Z-scheme system with another H_2-evolution photocatalyst is also an important way to achieve water splitting by Bismuth-based composite oxides. In this paper, a review about Bismuth-based composite oxides photocatalytic hydrogen generation is presented, mainly including the energy band engineering, Z-scheme overall water splitting and strategies for photocatalytic hydrogen generation activity improvement.

Energy band engineering

Several preparation methods were proposed to control conduction band minimum(CBM) and valence band maximum(VBM) of particle material, such as doping, quantum size effect, and solid solution. To realize photocatalytic hydrogen production by Bismuth-based composite oxides, it needs to improve their conduction band.

Doping elements

Generally, doping no matter metal or nonmetal ions can only introduce an intermediate energy level to narrow the energy band. For example, R. Asahi et al. found that Nitrogen-doped into substitutional sites of TiO_2 has proven to be indispensable for band-gap narrowing and photocatalytic activity [7]. Then, Tae Woo Kim et al. introduced Nitrogen to $BiVO_4$. It is found that nitrogen incorporation and oxygen vacancies of $BiVO_4$ not only effectively reduces the bandgap by ~0.2 eV but also increases the majority carrier density and mobility, enhancing electron-hole separation [79]. Therefore, doping fails to elevate CBM of Bismuth-based composite oxides satisfying the H^+/H_2. However, Cr doping into Bismuth-based composite oxides seems to be an exception. Cristiane G. Almeida et al. prepared pure and Cr(III) and Mo(V)-doped $BiNbO_4$ and $BiTaO_4$ by the citrate method. The metal doping influenced actively the crystal structure as well as the photocatalytic activity of the oxides. The photocatalytic activity in water splitting under visible light irradiation was evaluated by monitoring the H_2, CO_2 and CO evolution. The results showed that Cr(III)-doped $BiTaO_4$ and $BiNbO_4$ are more selective for hydrogen production, while Mo(V)-doped materials are more selective for CO_2 generation. By theoretical calculations, there is a slight shift of the CBM potential in Cr(III)-doped $BiTaO_4$ and $BiNbO_4$, as shown in Fig. 2 [66]. This CBM potential shift improves the reduction power of $BiTaO_4$ and $BiNbO_4$.

Additionally, Cr doped bismuth titanate also shows enhanced photocatalytic hydrogen production activity [64]. The improved photocatalytic performance of the Cr-modified $Bi_4Ti_3O_{12}$ is attributed to its strong absorption in the visible light region, small nanosheet size, exposed {001} facets as well as the low recombination rate or the high separation efficiency for photogenerated electron-hole pairs [65].

Quantum size effect

As we know, the band gap energy of a semiconductor is critically dependent on the particle size because of quantum size effect. G. P. Nagabhushana et al. reported for the first time a nanocrystalline *m*-$BiVO_4$ photocatalyst for H_2 evolution synthesized by a facile solution combustion synthesis method. The yield of hydrogen generated is about 489 μmol per 2.5 h of reaction under UV irradiation. The ultralight yellow crystalline combustion derived nanopowder exhibits porous morphology with strong absorption in the visible light region. The estimated band gap of *m*-$BiVO_4$ powder is about 2.52 eV. The H_2 evolution and photocatalytic activity of *m*-$BiVO_4$ nanocrystalline powder can be attributed to its physical properties such as nanosize particles and large surface area, as shown in Fig. 3 [67].

Then, Sun et al. also reported quantum sized $BiVO_4$ could decompose pure water into H_2 and O_2 simultaneously under simulated solar light irradiation without any cocatalysts or sacrificial reagents. The valence band edge position of the quantum-sized $BiVO_4$ was almost identical with that of the nanoscale sample, which may be the origin of the similar water

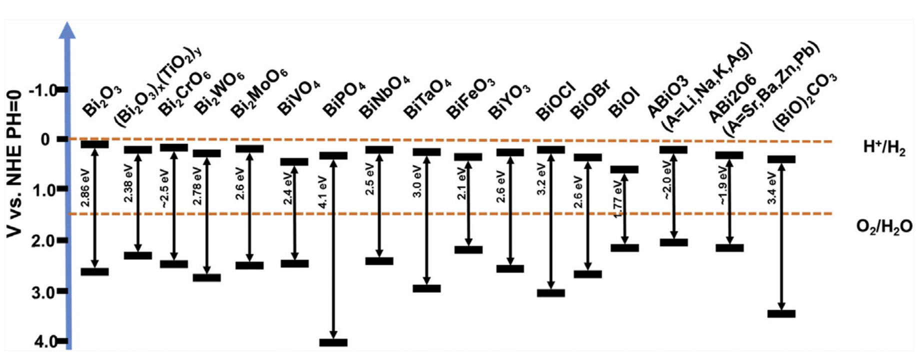

Fig. 1 — Band positions of Bismuth-based composite oxides [21–51].

Please cite this article as: Fang W, Shangguan W, A review on bismuth-based composite oxides for photocatalytic hydrogen generation, International Journal of Hydrogen Energy, https://doi.org/10.1016/j.ijhydene.2018.11.063

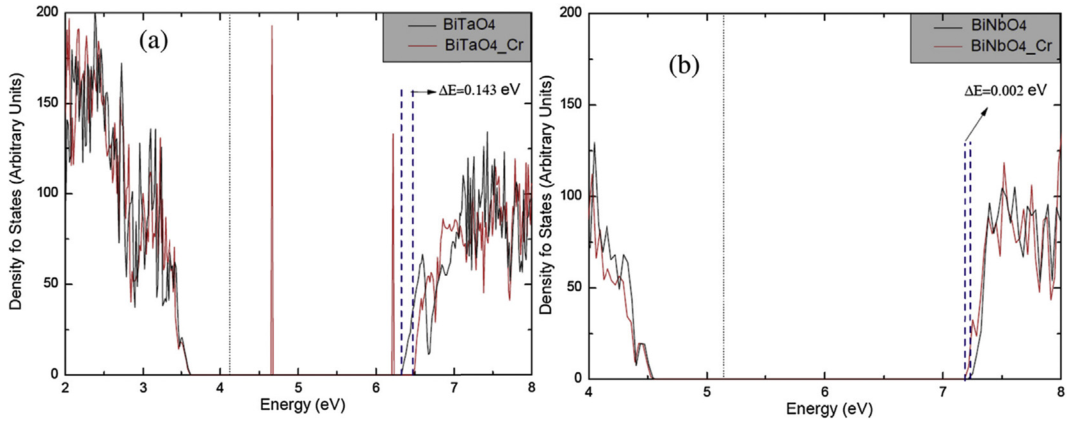

Fig. 2 – Density of states of the Cr-doped $BiTaO_4$ (a) and$BiNbO_4$ (b) [66].

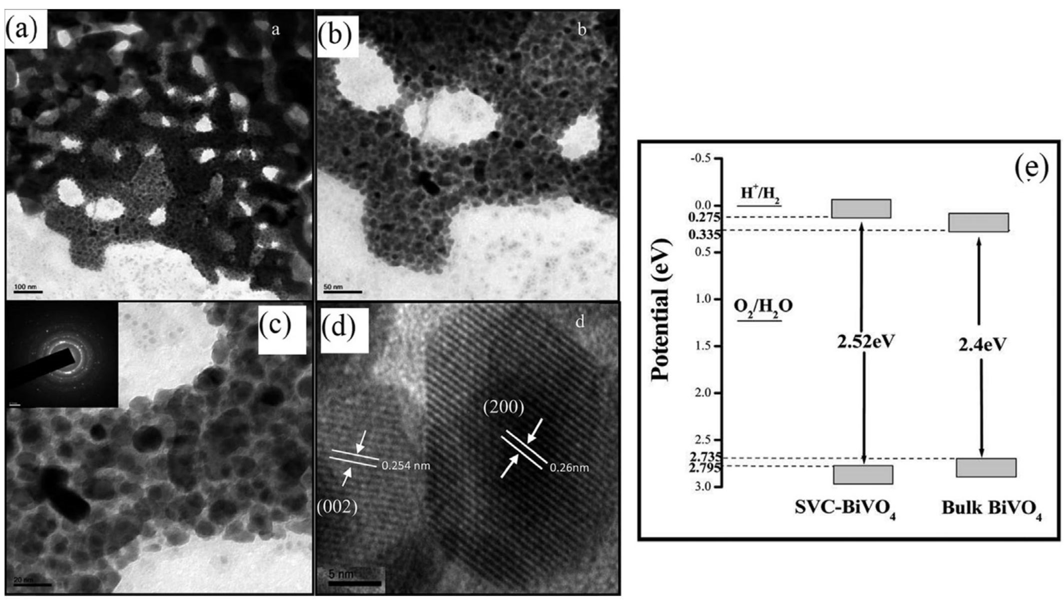

Fig. 3 – (a–c) TEM, (inset of C) SAED pattern, (d) HRTEM images of small volume combustion SVC-$BiVO_4$. (e) Potential energy diagram for the photochemical reaction of SVC-$BiVO_4$ [67].

oxidation potential on different $BiVO_4$ samples. Considering the difference in the band gap is about 0.3 eV between the nano-scale and quantum sized samples from their absorption spectra, the negative shift of CBM for quantum sized $BiVO_4$ may be more than 0.1 eV because the valence band position is almost the same, as shown in Fig. 4 [68]. However, the detailed mechanism of water splitting with quantum sized $BiVO_4$ and the nonstoichiometric ratio of H_2 and O_2 are not clear.

The preparation methods and conditions of quantum sized Bismuth-based composite oxides are harsh. Zhihua Sun et al. designed a method where Graphene oxide (GO) served as the support on which Bi_2WO_6 formed in situ [70]. Bi_2WO_6 nanoparticles with the size of 30–40 nm were homogeneously dispersed on the surface of graphene sheets, due to their bonding with graphene as shown in Fig. 5(a) [70]. More interestingly, H_2-production by Gr- Bi_2WO_6-T was also observed to be as high as 159.20 μmol/h. The improved effectively could be ascribed to the existence of the graphene that led to decrease in conduction band potential and resulted in a more negative reduction potential than H^+/H_2, shown in Fig. 5(c). Bao Pan et al. also found that the incorporation of RGO into $BiPO_4$ significantly enhanced the photocatalytic activity for H_2 evolution, and the photocatalytic activity increases in the order of $BiPO_4$/RGO-hydrothermal> $BiPO_4$/RGO-photoreduction> $BiPO_4$/RGO-hydrazine [69].

Solid solution

Except for quantum size effect, the solid solution has also been proved to be an effective method to regulate the energy band. Solid solution has a series of different band gaps because its components can change in a big proportional band. So it is a feasible and effective method to obtain suitable CB and VB for water splitting.

Bi_2O_3

Jia Yang et al. developed an oxide photocatalyst $Bi_2Ga_4O_9$ (loaded with RuO_x) capable of overall water splitting under

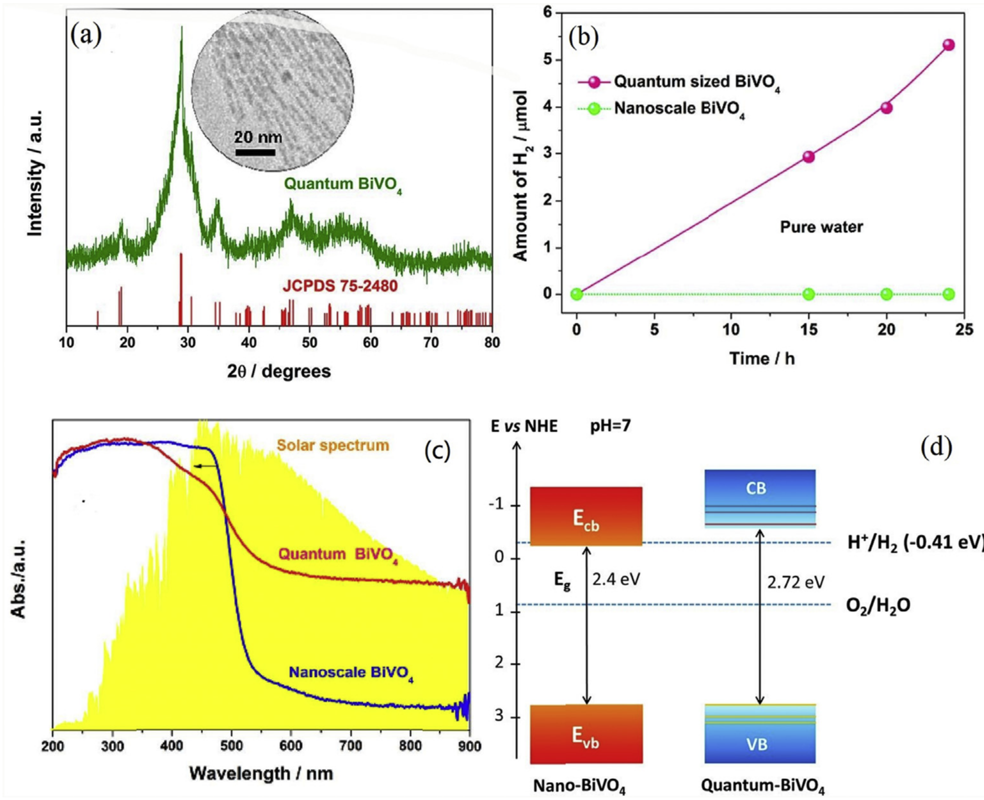

Fig. 4 – (a) HRTEM image and XRD pattern of the synthetic quantum sized $BiVO_4$; (b) Hydrogen evolution from 15 mg of $BiVO_4$ samples in pure water; (c) UV–vis diffuse reflection spectra of the quantum-sized $BiVO_4$ and nanoparticles; (d) Schematic band structures of nanoscale $BiVO_4$ and quantum sized $BiVO_4$ [68].

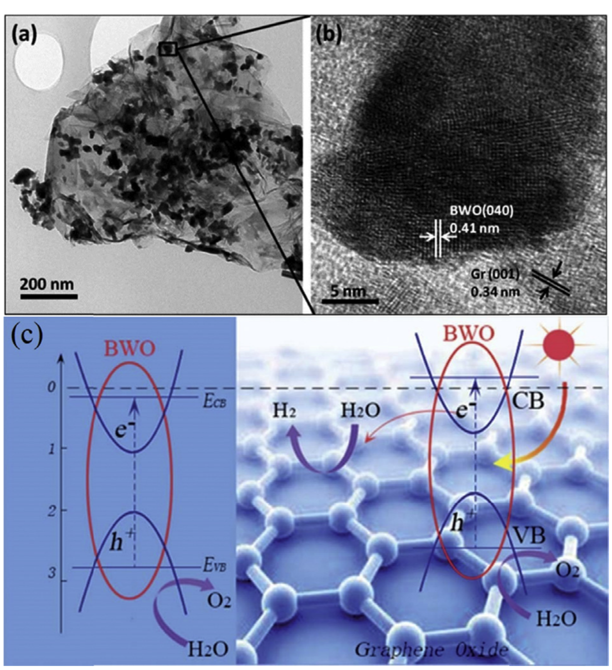

Fig. 5 – (a) and (b) TEM images of Gr–Bi_2WO_6-T at different resolutions; (c) Schematic description of the mechanism of the photocatalytic activity in Gr- Bi_2WO_6-T [70].

visible light, with the rationale of combining Bi^{3+} and Ga^{3+} [55]. For comparison, the estimated CB and VB potentials for Ga_2O_3, Bi_2O_3, and $Bi_2Ga_4O_9$ according to the Mulliken electronegativity were shown in Fig. 6. The bandgap for Ga_2O_3 is wide enough for water splitting, but only in response to UV light irradiation. Bi_2O_3 possesses the narrowest bandgap among these three compounds and is active under visible light. The drawback is also obvious that it is thermodynamically incapable of water reduction. When combining Bi^{3+} and Ga^{3+}, $Bi_2Ga_4O_9$ can obtain appropriate CB and VB potentials for overall water splitting.

Bismuth titanate $(Bi_2O_3)_x(TiO_2)_y$ is a photoactive member of the pyrochlore family that can potentially meet the objectives above desired of a photocatalyst. Sankaran Murugesan et al. reported a simple and robust template-free reverse micelle method to synthesize highly crystalline stoichiometric bismuth titanate nanorods which display a marked red shift about 48 nm compared to P25, as shown in Fig. 7 [53]. The $Bi_2Ti_2O_7$ nanorods demonstrate improved photocatalytic hydrogen generation, which also shows visible light activity.

Bi_2WO_6

Liu et al. first use Y element to raise the CBM of Bismuth-based composite oxides [40]. It is found that $BiYWO_6$ (BYW) oxide solid solution can act as a photocatalyst for overall water

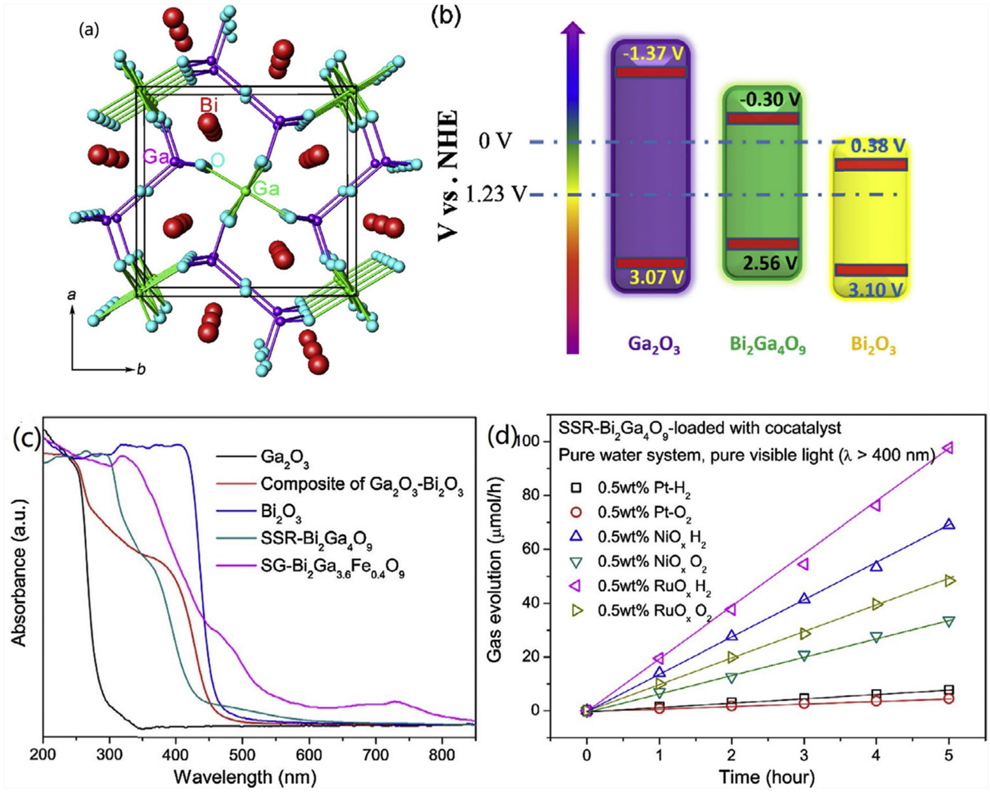

Fig. 6 — (a) Crystal structure view of mullite- $Bi_2Ga_4O_9$ along the c-axis; (b) schematic view of the estimated CB and VB potentials for Ga_2O_3, Bi_2O_3, and $Bi_2Ga_4O_9$ according to the Mulliken electronegativity; (c) UV–vis absorption spectra for SSR-Bi_2Ga4O_9 and SG-$Bi_2Ga_{3.6}Fe_{0.4}O_9$, and for comparison, the spectra for Bi_2O_3, Ga_2O_3, and mechanically mixed Ga_2O_3–Bi_2O_3;(d) Time-dependent H_2 and O_2 evolution over SSR-$Bi_2Ga_4O_9$ loaded with various co-catalysts in a pure water system. Conditions: 50 mg of photocatalyst in pure water (50 mL), λ > 400 nm [55].

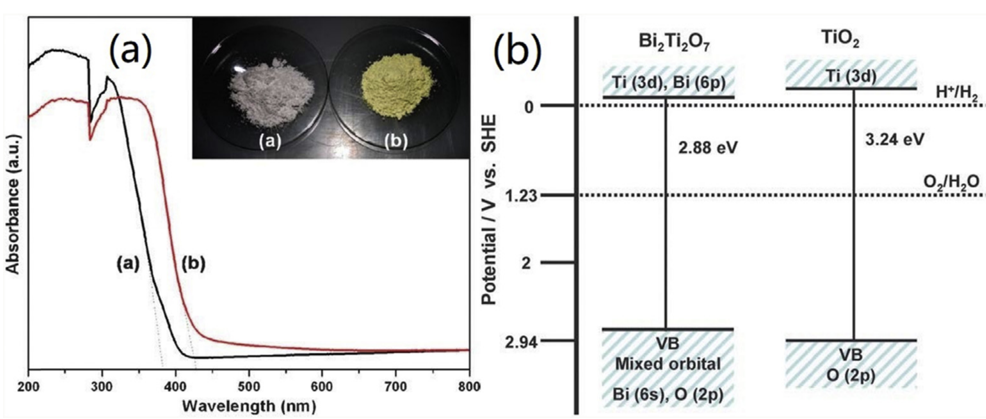

Fig. 7 — (a) Comparison of the diffuse reflectance (DR) measurements of commercial TiO_2 (P25) with $Bi_2Ti_2O_7$ nanorods; (b) Schematic representation of band edges of $Bi_2Ti_2O_7$ pyrochlore nanorods and TiO_2 from DR UV–vis and DFT calculations [53].

splitting under the visible light when loading cocatalysts. The band gap of BYW was 2.71 eV, and it absorbed visible light up to 470 nm. BYW with RuO_2 has the best activity compared to other cocatalysts such as Cr_2O_3–Pt, Pt, and Au. Under irradiation of λ > 420 nm light, the amounts of the produced hydrogen and oxygen were about 12.3 and 5.6 μmol in 3 h, respectively, shown in Fig. 8. This study indicated that the formation of the solid solution was the feasible method to adjust the conduction band and valence band to obtain a visible-light-driven photocatalyst.

$BiVO_4$

Then, a series of mixed oxide photocatalysts $Bi_xY_{1-x}VO_4$ (BYV) were prepared by solid-state reaction. When the composition was below x = 0.65, $Bi_xY_{1-x}VO_4$ were of single phase and zircon-type structure and can be regarded as solid solutions of

Please cite this article as: Fang W, Shangguan W, A review on bismuth-based composite oxides for photocatalytic hydrogen generation, International Journal of Hydrogen Energy, https://doi.org/10.1016/j.ijhydene.2018.11.063

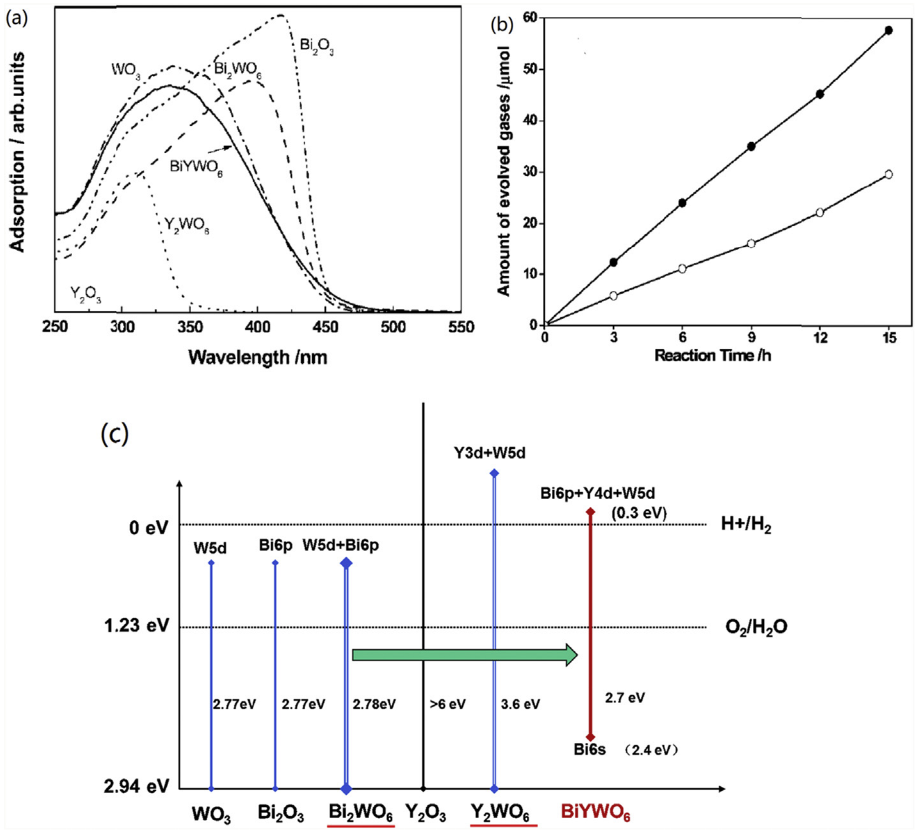

Fig. 8 – (a) Diffuse Reflection Spectra of $BiYWO_6$, Bi_2O_3, Y_2O_3, WO_3, Bi_2WO_6, and Y_2WO_6 samples; (b) Amounts of H_2 and O_2 produced on 0.5 wt % RuO_2– $BiYWO_6$ under visible light irradiation (>420 nm); (c) scheme for band positions [40].

YVO_4 and $BiVO_4$ within the same structure. All the $Bi_xY_{1-x}VO_4$ solid solutions were proved for the first time to be effective photocatalysts based on Bi with d^0 electron configuration for overall water splitting under UV light, as shown in Fig. 9. Among all the samples, $Bi_{0.5}Y_{0.5}VO_4$ with Rh–Cr_2O_3 cocatalyst showed the highest photocatalytic activity (402 μmol/h H_2 and 196 μmol/h O_2). Under visible light irradiation, $Bi_{0.5}Y_{0.5}VO_4$ solid solutions also performed a photocatalytic activity to produce H_2 and O_2 from sacrificial reagent solutions. The photocatalytic activity of $Bi_xY_{1-x}VO_4$ solid solutions was effectively improved by increasing calcination temperature from 1073 to 1173 K. Additionally, the effect of pH on the photocatalytic activity are shown in Fig. 9(e). It is found strong alkaline and acidic conditions are adverse to water splitting.

Band structure calculation by using the WIEN2K code indicated that incorporation of Bi in YVO_4 caused a reduction of the band gap and dispersion of the conduction band of $Bi_xY_{1-x}VO_4$ solid solution due to the interaction between Bi6s/6p and VO_4, which was demonstrated to be the major factor for the effective activity of $Bi_xY_{1-x}VO_4$ solid solutions. Moreover, the Crystal structures, Morphology and surface chemical state of $Bi_xY_{1-x}VO_4$ solid solutions were unchangeable in the process of photocatalytic water splitting.

Furthermore, $Bi_{0.5}M_{0.5}VO_4$ (BMV; M = La, Eu, Sm, Dy, and Y) solid solutions were prepared and studied [72,74]. All the samples were proved to produce H_2 and O_2 simultaneously from pure water under the irradiation of UV light. M – O bond lengths were proved to increase with M cations by refining cell parameters and atomic positions. Besides, band gaps, energy gaps and photocatalytic activities of BMV also changed with M cations. Both of M–O and V–O bond lengths were suggested to account for this phenomenon. Inactive $A_{0.5}Y_{0.5}VO_4$ (A = La, Ce) for water splitting proved incorporation of Bi rather than a distortion of VO_4 tetrahedron was a critical factor for improving the efficiency of overall water splitting by facilitating the generation of electron and hole with lighter effective masses, as shown in Fig. 10. Replacement of Bi by M cations not only gave indirect effect on band structure but also raised the position of conduction band minimum to meet the requirement of H_2 production.

Others

Other complicated Bismuth-based composite oxides constructed by solid solution were also proved to be capable of photocatalytic hydrogen production from water splitting, such as: $Sr_{1-x}Bi_xTi_{1-x}Fe_xO_3$ [63], $CuBi_2O_4$ [62], Bi_4NbO_8Cl [60], Bi_4YNbO_8Cl [61], $Na(Bi_xTa_{1-x})O_3$ [57], $Bi_{0.5}Na_{0.5}TiO_3$ [56], Bi_3NbO_7 [58] shown in Table 1.

Z-scheme overall water splitting

Bismuth-based composite oxides are always used as O_2-evolution photocatalysts in the Z-scheme system to achieve overall water splitting. Hideki Kato et al. developed the Z-scheme system to achieve water splitting under visible light

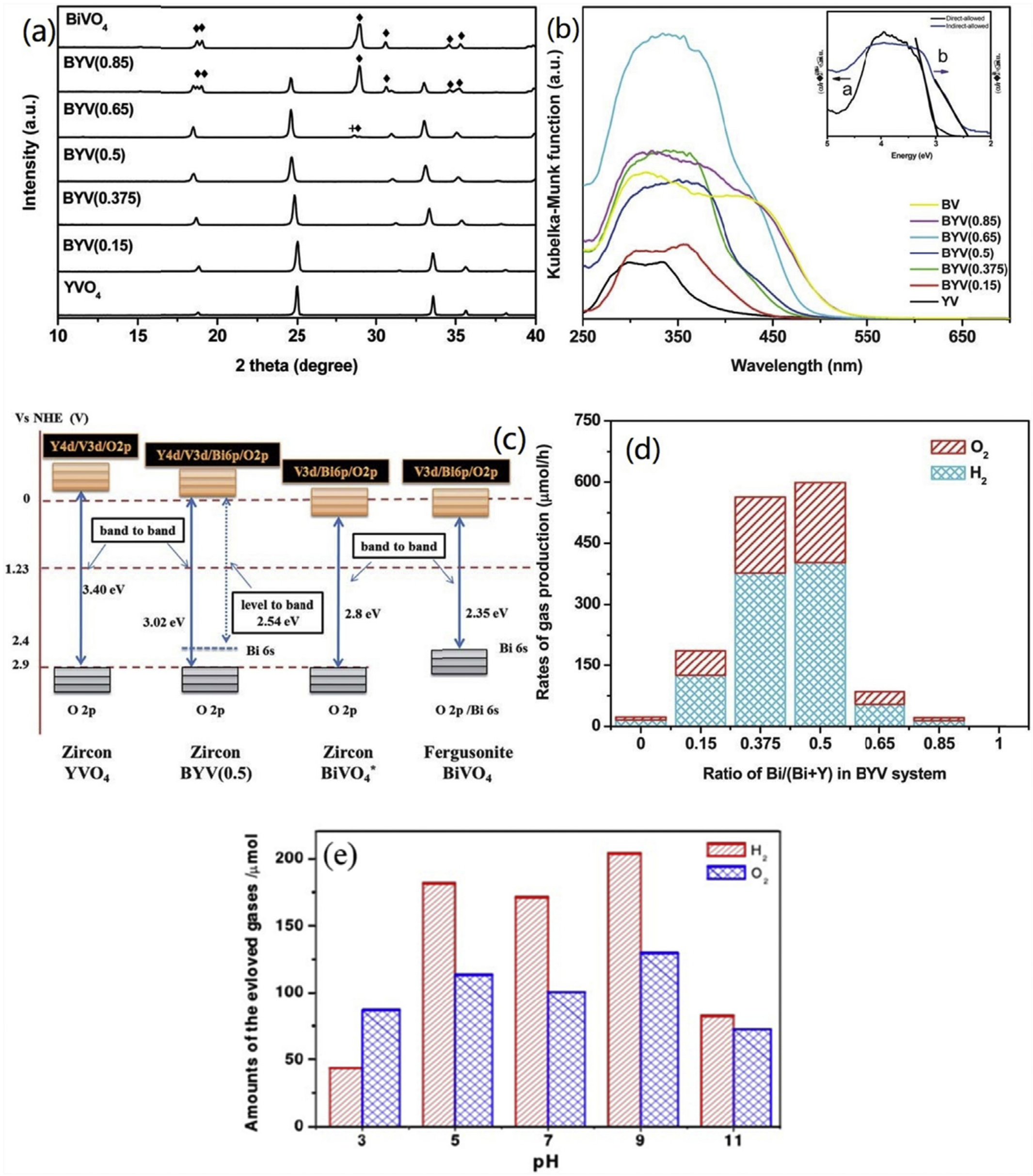

Fig. 9 – (a) Powder X-ray diffraction patterns of $Bi_xY_{1-x}VO_4$ mixed oxides; (b) Diffuse reflectance UV–Vis spectra of the $Bi_xY_{1-x}VO_4$ mixed oxides; (c) Schematic band structures of YVO_4, BYV(0.5), zircon type $BiVO_4$ and fergusonite $BiVO_4$; (d) Photocatalytic activities of BYV mixed oxides loaded with Rh–Cr_2O_3 co-catalyst for water splitting under full arc-light irradiation [73]; (e) Overall water splitting under different pH on BYV(0.5).

irradiation, which constituted of a Fe^{3+}/Fe^{2+} redox couple as an electron relay and two powdered heterogeneous photocatalysts, as shown in Fig. 11 [80]. The (Pt/$SrTiO_3$:Rh)–($BiVO_4$) system showed the highest activity with 0.3% of an apparent quantum yield at 440 nm. It can use visible light up to 520 nm.

However, the photocatalytic activity of the system using the Pt co-catalyst decreased as the partial pressures of evolved H_2 and O_2 were increased. Then, they use a Ru as co-catalyst for overall water splitting which was as high as that of the system using a Pt co-catalyst. In contrast, such deactivation was not observed for the system using the Ru co-catalyst. The investigation of the back-reaction revealed that water formation from H_2 and O_2, reduction of Fe^{3+} by H_2, and oxidation of Fe^{2+} by O_2 were significantly suppressed in the system using the Ru co-catalyst, resulting in good photocatalytic performance for water splitting. The (Ru/$SrTiO_3$:Rh)-($BiVO_4$)-(Fe^{3+}/Fe^{2+}) photocatalysis system gave a quantum yield of 0.3% and a stable activity more than 70 h [81].

The electron mediator used in the Z-scheme system always gives adverse effects, such as backward-reactions of water splitting and the shielding of incident light. Moreover, Kudo et al. reported a new type of Z-scheme photocatalyst system driven by interparticle electron transfer (IPET) between an H_2-evolving photocatalyst (Ru/$SrTiO_3$:Rh) and an O_2-evolving photocatalyst ($BiVO_4$) without an electron mediator. The $BiVO_4$–Ru/$SrTiO_3$:Rh composite photocatalyst gave a

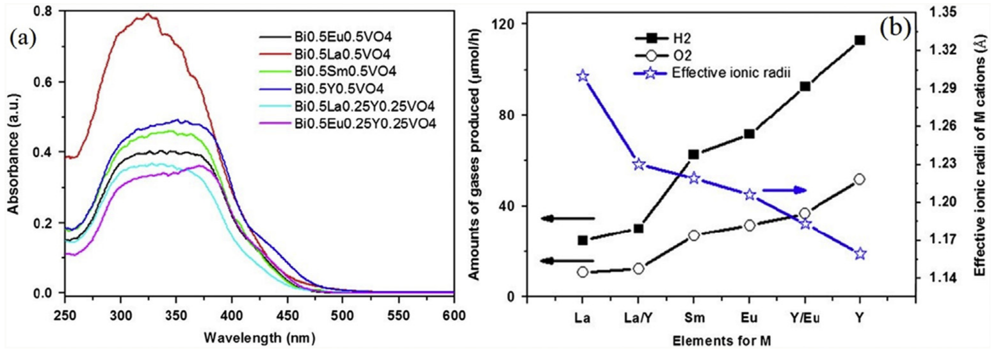

Fig. 10 – (a) UV–visible diffuse reflectance spectra of BMV solid solutions; (b) Photocatalytic activities of BMV solid solutions and effective ionic radii of M cations [74].

Table 1 – Bismuth-based composite oxides for photocatalytic hydrogen production.

Photocatalysts	Cocatalysts	Activity		Test condition	References
		H_2	O_2		
$Bi_2Ti_2O_7$	none	285 ml	none	methanol-water	[53]
Bi_3NbO_7	NiO (1.5 wt%)	110.7 μmol/h/g	none	methanol-water >420 nm	[54]
$Bi_2Ga_4O_9$	RuO_x	19.3 μmol/h/g	9.7 μmol/h/g	Pure water >400 nm	[55]
$Bi_{0.5}Na_{0.5}TiO_3$	Pt	325.4 μmol/h/g	none	methanol-water	[56]
$Na(Bi_xTa_{1-x})O_3$	NiO	75 μmol/h/g	none	methanol-water >400 nm	[57]
Bi doped $NaTaO_3$	Pt	0.86 μmol/h/g	none	methanol-water >390 nm	[58]
BiOI	none	1316.9 μmol/h/g	~650 μmol/h/g	Pure water >400 nm	[59]
Bi_4NbO_8Cl	Pt	0.1 μmol/h	none	methanol-water >300 nm	[60]
$Bi_2Y_2NbO_8Cl$	Pt	113 μmol/h	none	$C_6H_{12}O_6$-water >380 nm	[61]
$CuBi_2O_4$	none	16 μmol/h	none	KI solution	[62]
$Sr_{1-x}Bi_xTi_{1-x}Fe_xO_3$	Pt	50 μmol/h	none	sodium sulfite aqueous solution	[63]
$Bi_4Ti_{2.6}Cr_{0.4}O_{12}$	NiO_x	100 μmol/h/g	None	methanol-water >400 nm	[64]
$Bi_4Ti_{2.6}Cr_{0.4}O_{12}$	none	117 μmol/h/g	none	methanol-water >420 nm	[65]
Cr-doped $BiNb(Ta)O_4$	Pt	7 μmol/h/g	none	30% isopropanol >418 nm	[66]
$BiVO_4$	none	195.6 μmol/h	none	Water–ethanol	[67]
quantum $BiVO_4$	none	0.22 μmol/h	–	Pure water	[68]
$BiPO_4$/RGO	none	30.6 μmol/h	none	ethanol aqueous solution	[69]
Bi_2WO_6–graphene	none	952.38 μmol/h	none	lactic acid	[70]
$BiYWO_6$	1 wt% Pt–Cr2O3	51.4 μmol/h	24.6 μmol/h	Pure water >300 nm	[40]
$Bi_{0.5}Dy_{0.5}VO_4$	0.1 wt% Pt–Cr_2O_3	33.7 μmol/h	17.6 μmol/h	Pure water >300 nm	[71,72]
$Bi_xY_{1-x}VO_4$	0.275 wt% Rh-0.4 wt% Cr_2O_3	402 μmol/h	196 μmol/h	Pure water >300 nm	[73–77]
$Bi_{1-x}Sm_xVO_4$	Pt/Cr_2O_3	188.25 μmol/h/g	95.90 μmol/h/g	Pure water >300 nm	[78]

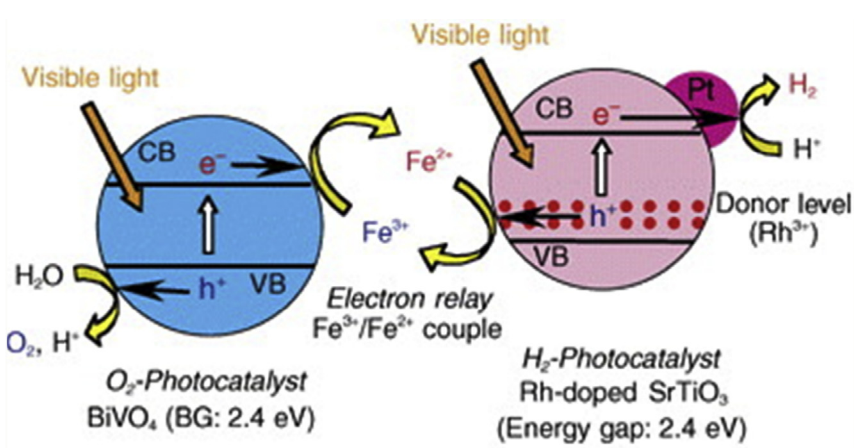

Fig. 11 – Mechanism of overall water splitting using a Z-scheme photocatalysis system [80].

Please cite this article as: Fang W, Shangguan W, A review on bismuth-based composite oxides for photocatalytic hydrogen generation, International Journal of Hydrogen Energy, https://doi.org/10.1016/j.ijhydene.2018.11.063

quantum yield of 1.6% at 420 nm and a stable activity [82,83]. Additionally, reduced graphene oxide, Carbon dots, and Au are also demonstrated to be the effectiveness of as a solid electron mediator for water splitting in the Z-scheme photocatalysis system [3,84–87]. Especially, Qian Wang et al. presented photocatalyst sheets based on La– and Rh-codoped $SrTiO_3$ ($SrTiO_3$:La,Rh) and Mo-doped $BiVO_4$ ($BiVO_4$:Mo) powders embedded into gold (Au) layer. Enhancement of the electron relay by annealing and suppression of undesirable reactions through surface modification allows pure water (pH 6.8) splitting with a solar-to-hydrogen energy conversion efficiency of 1.1% and an apparent quantum yield of over 30% at 419 nm, as shown in Fig. 12 [3].

The above Z-scheme photocatalysis systems are all used $SrTiO_3$:Rh for H_2 evolution and $BiVO_4$ for O_2 evolution. Qin et al. report that zinc-doped (10%) g-C_3N_4 and $BiVO_4$ can also construct the Z-scheme photocatalysis system [88]. Hironori Fujito showed that the layered oxychloride Bi_4NbO_8Cl with the Sillen–Aurivillius perovskite works as a stable photocatalyst for water oxidation under visible light, which can enable a Z-scheme overall water splitting by coupling with an H_2-evolving photocatalyst (Rh-doped $SrTiO_3$) [60].

Strategies for photocatalytic hydrogen generation activity improvement

The general principles to improve the photocatalytic hydrogen generation activity Including 1) increase visible light absorption; 2) promote the separation of photogenerated electron-hole pairs; 3) shorten the photogenerated electron-hole mobility distance; 4) increase active sites. Draw on past achievements and experience in the study of TiO_2, CdS, and $BiVO_4$, many strategies can also be adopted for Bismuth-based composite oxides. Among them, Crystal facet engineering, Surface modification, and efficient cocatalysts are widely studied.

Crystal facet engineering

It is thought that single inorganic crystals with different highly reactive surfaces exposed are important for photocatalytic reaction. Unfortunately, surfaces with high reactivity usually diminish rapidly during the crystal growth process as a result of the minimization of surface energy [89]. Teruhisa Ohno et al. firstly studied a titanium dioxide powder consisting of 1 μm size rutile and anatase particles [90]. By SEM, it was found that the rutile particles exposed {011} and {110} crystal faces, and the anatase particles exposed {001} and {011} faces. Though in situ photoinduced Pt and PbO_2 on this titanium dioxide powder, Pt was observed mostly on the {110} face of rutile particles and the {011} face of anatase particles, while PbO_2 were observed on the {011} face of the rutile particles and the {001} face of the anatase particles, as shown in Fig. 13. These results indicate that the crystal faces help in the separation of electrons and holes.

Then, Huagui Yang et al. further modulation the ratio of {011} and {001} [89]. They found that for fluorine-terminated surfaces this relative stability is reversed: {001} is energetically preferable to {101}. Uniform anatase TiO_2 single crystals with a high percentage (47%) of {001} facets are synthesized successfully. And then, Pan et al. investigated a set of anatase crystals with predominant {001}, {101}, or {010} facets. Contrary to conventional understanding, clean {001} exhibits lower reactivity than {101} in photooxidation reactions for OH radical generation and photoreduction reactions for hydrogen evolution. Furthermore, the {010} facets showed the highest photoreactivity [91]. Thomas R. Gordon et al. also estimated that higher percentages of {101} facets correlate with higher photocatalytic activity, as shown in Fig. 14 [92].

Except TiO_2, $BiVO_4$ exposed with {010} and {110} crystal facets also show different redox property. Water oxidation activity is increased when photodeposition of reduction cocatalysts on {010} facets and oxidation cocatalysts on {110} facets [93]. Tachikawa et al. investigated the reaction dynamics of the photo and electrically generated charges on the specific crystal facets of $BiVO_4$. The trapped holes are preferentially located on the lateral {110} facets of the $BiVO_4$ crystal, while the electrons are uniformly distributed over the crystal, as shown in Fig. 15 [94].

Recently, Unprecedented 30-faceted $BiVO_4$ polyhedra predominantly surrounded by {132}, {321}, and {121} high-index facets are fabricated through the engineering of high-index surfaces by a trace amount of Au nanoparticles [95]. The growth of high-index facets results in a 3–5 fold enhancement of O_2 evolution from photocatalytic water splitting by the $BiVO_4$ polyhedron, relative to its low-index counterparts.

Based on the studies above, Fang et al. successfully synthesized $Bi_xY_{1-x}VO_4$ solid solution by hydrothermal method. The $Bi_xY_{1-x}VO_4$ has a new dodecahedron shape with two

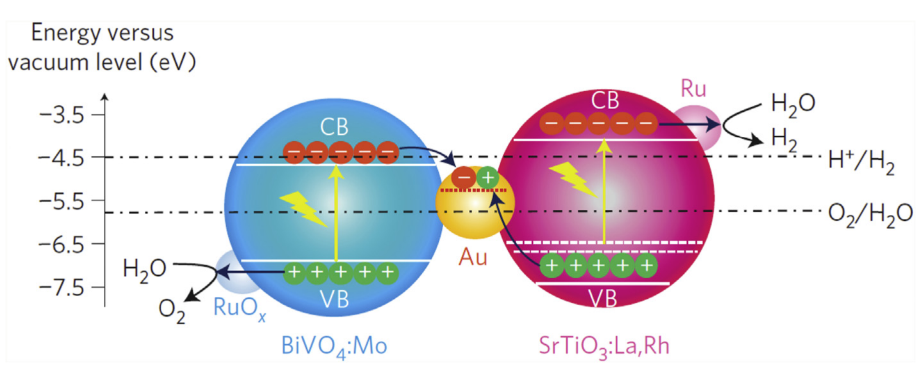

Fig. 12 – Schematic of overall water splitting on the Ru-modified $SrTiO_3$:La,Rh/Au/$BiVO_4$:Mo sheet [3].

Please cite this article as: Fang W, Shangguan W, A review on bismuth-based composite oxides for photocatalytic hydrogen generation, International Journal of Hydrogen Energy, https://doi.org/10.1016/j.ijhydene.2018.11.063

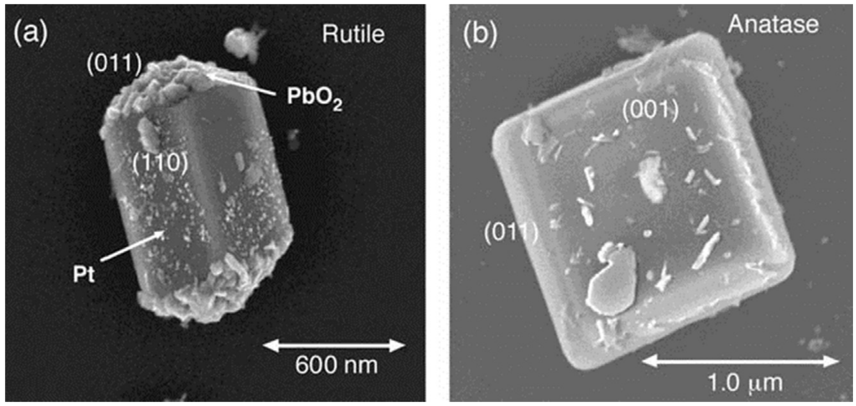

Fig. 13 – SEM images of a rutile particle (a) and an anatase particle (b) showing PbO_2 deposits, which were loaded on the particles by UV irradiation of the Pt-deposited TiO_2 powder in a solution of 0.1 M $Pb(NO_3)_2$. Prior to the deposition of PbO_2, Pt fine particles were deposited on the TiO_2 particles by a photocatalytic reaction in a solution containing 1.0 mM H_2PtCl_6 and 0.52 M 2-propanol [90].

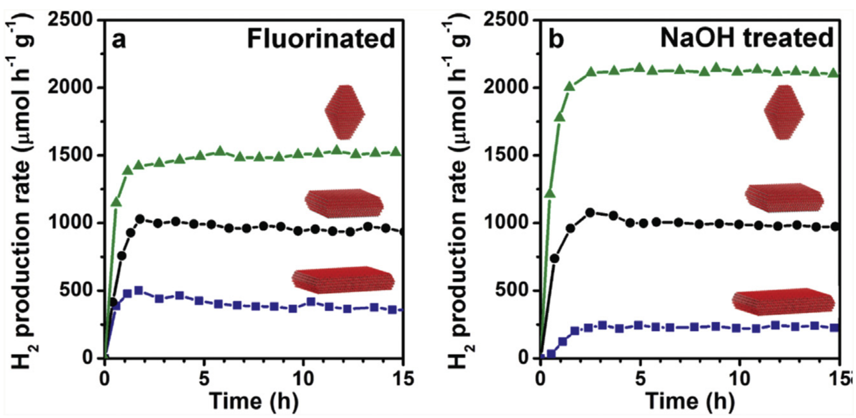

Fig. 14 – Hydrogen production rate from 1 wt % Pt loaded samples of ligand-exchanged, (a) fluorinated and (b) NaOH-treated TiO_2 NCs under solar illumination in 1:1 mixtures of $MeOH/H_2O$ [92].

facets {101} and {100} exposed. Among the facets {100} in $Bi_xY_{1-x}VO_4$ with tetragonal zircon structure, (100), (−100), (010) and (0−10) are identical. And facets {101} and {100} have lower surface energies under acidic condition. Thus, the dodecahedron is made up of eight {101} faces and four {100} faces. Through studying photocatalytic water splitting over $Bi_xY_{1-x}VO_4$ with the Pt as co-catalyst, $Bi_{0.5}Y_{0.5}VO_4$ can split water with stoichiometric ratio steadily. Rates of H_2 and O_2 production are 164.5 μmol/h and 83 μmol/h respectively. Moreover, with $NaNO_2$ filter (λ > 400 nm), $Bi_{0.5}Y_{0.5}VO_4$ can also split pure water with H_2 production about 1 μmol/h. By experiment and calculation, efficient charge separation achieved on facets {101} and {100} plays a vital role in water splitting with the stoichiometric ratio, as shown in Fig. 16 [75].

Surface modification

Though crystal facet engineering, photocatalysts can selectively expose some highly reactive surfaces. To further improve photocatalytic hydrogen generation activity, it needs to explore the property of each surface due to the photochemical reaction occurs on the exposed surfaces. Photocatalytically favorable surface should contain a large fraction of uncoordinated surface atoms and expose more active sites.

Among them, an oxygen vacancy is most widely studied, which play an important role in mediating the interfacial electron transfer and thus photocatalytic activity. The $BiPO_{4-x}$ nanorod with surface oxygen vacancy was fabricated via vacuum deoxidation. The photocatalytic activity depended on the concentration and kind of surface oxygen vacancy, and the optimum photocatalytic activity and photocurrent of the $BiPO_{4-x}$ nanorod were about 1.5 and 2.5 times as high as that of pure $BiPO_4$, respectively [45]. Oxygen vacancies can also improve the solar absorption and donor density significantly. Oxygen-deficient BiOI nanosheets exhibit an unexpected redshift of about 100 nm in the light absorption band and one order of magnitude improvement in donor density compared to the untreated BiOI nanosheets [96]. Moreover, Vacancy-rich layered materials have good electron transfer property. Jun Li et al. studied the vacancy-rich monolayer BiO_{2-x}. Compared to bulk BiO_{2-x}, monolayer BiO_{2-x} exhibited enhanced photocatalytic performance for Rhodamine B and phenol removal under UV, visible and near-infrared light (NIR) irradiation,

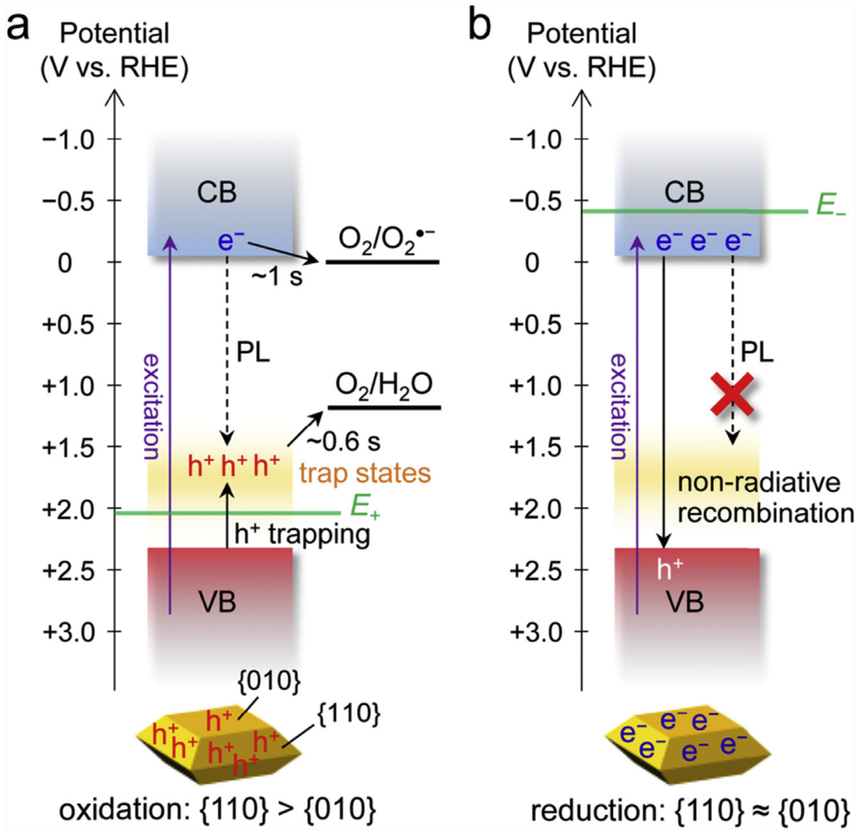

Fig. 15 — Schematic diagram showing the energy band structure of $BiVO_4$ and related charge transfer processes under positive (a) and negative (b) potentials [94].

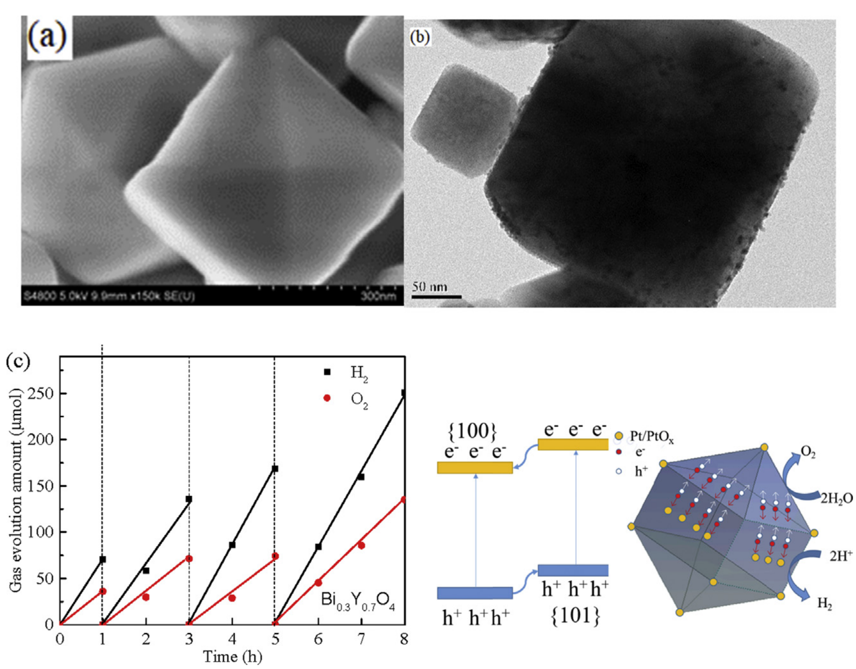

Fig. 16 — (a) SEM of the dodecahedron $Bi_xY_{1-x}VO_4$; (b) HRTEM of the samples loading with Pt (1 wt%); (c) the reaction was carried out under Xe lamp (300W) illumination by Pt (1 wt%)-$Bi_{0.3}Y_{0.7}VO_4$; (d) sketch for the transfer process of photo-generated charges [75].

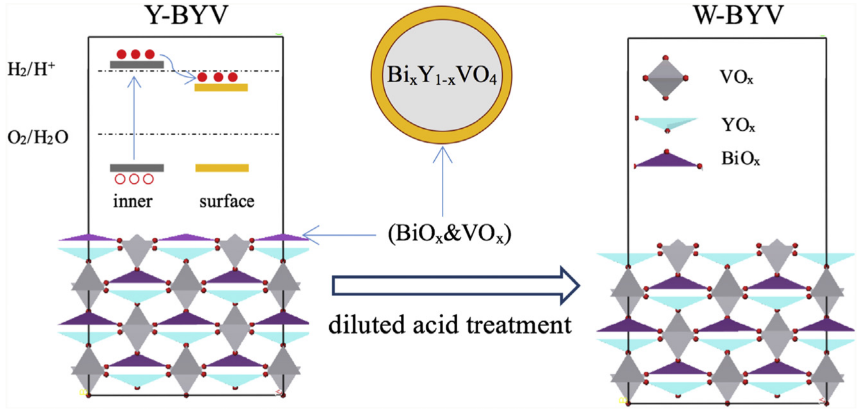

Fig. 17 — Scheme diagram for enhanced photocatalytic water splitting activity of $Bi_xY_{1-x}VO_4$ solid solution by diluted acid treatment [72].

attributed to the vacancy associates V_{Bi-O}. The presence of V_{Bi-O} defects in monolayer BiO_{2-x} promoted the separation of electrons and holes [97]. Kaining Ding et al. explore the origin of the enhanced photocatalytic activity of Mo-doped monoclinic $BiVO_4$. They found that Mo doping on the surface can result in surface oxygen quasi-vacancies and enhance the exposure of surface Bi atoms, which is confirmed to improve the adsorption of water molecules [98]. Additionally, oxygen vacancies can be created by plentiful V^{4+} species, which can adsorb Rhodamine B before irradiation owing to the appearance of plentiful O_2 and OH species on the surface [99]. Marta D. Rossell further provides direct evidence for the segregation of oxygen vacancies at the surface of $BiVO_4$ using electron energy-loss spectroscopy in scanning transmission electron microscopy. Within a 5-nm-thick shell, the oxidation state of vanadium is reduced from +5 to +4. Thus, charge neutrality near the surface demands for ~15% oxygen vacancies [100].

Except for surface oxygen vacancy, it is found other elements' chemical state also affect the photocatalytic activity. Fang et al. found that the surface properties of yellow-$Bi_xY_{1-x}VO_4$(Y-BYV) and yellow-$Bi_xY_{1-x}VO_4$(W-BYV), especially surface chemical composition, play an important role in the photocatalytic activity. BiO_x, YO_x, and VO_x are distributed randomly on the surface of $Bi_xY_{1-x}VO_4$ without diluted acid treatment [72]. The color of $Bi_xY_{1-x}VO_4$ changes with the amount of BiO_x on the surface. As we know, the conduction band of BiO_x is lower than that of H_2O/H_2. As a result, the photo-generated electrons prefer to migrate to the lower

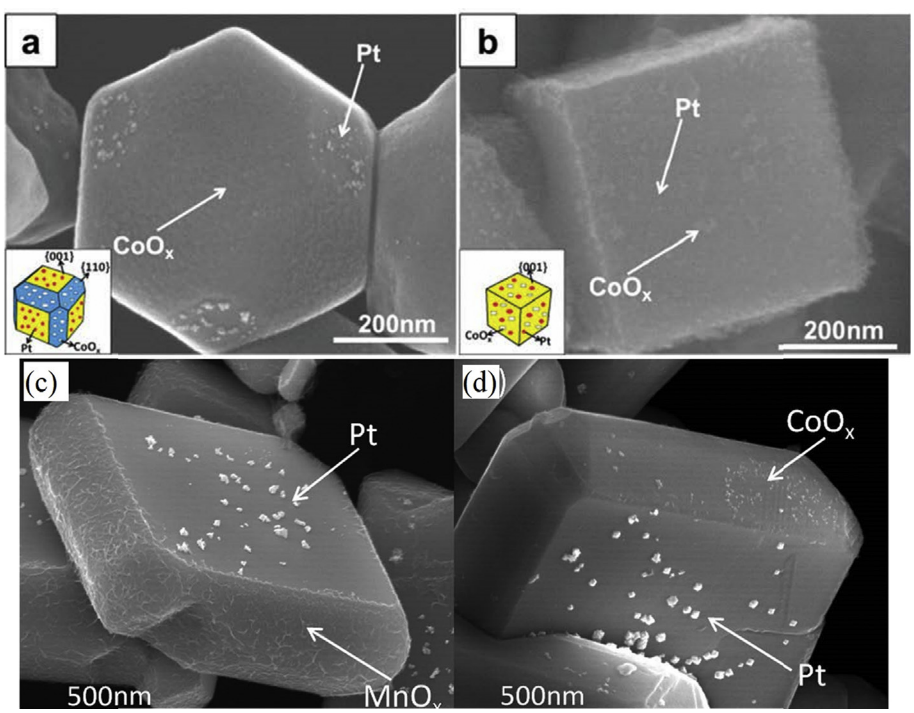

Fig. 18 — The SEM images of the 18-facet, 6-facet $SrTiO_3$ and 10-facet $BiVO_4$ nanocrystals with simultaneous photodeposition of Pt and Co_3O_4 as cocatalysts. (a) Pt–Co_3O_4/18-facet $SrTiO_3$ and (b) Pt–Co_3O_4/6-facet $SrTiO_3$; (c) Pt (P.D.)/MnO_x (P.D.)/$BiVO_4$; (d) Pt (P.D.)/Co_3O_4 (P.D.)/$BiVO_4$ [93].

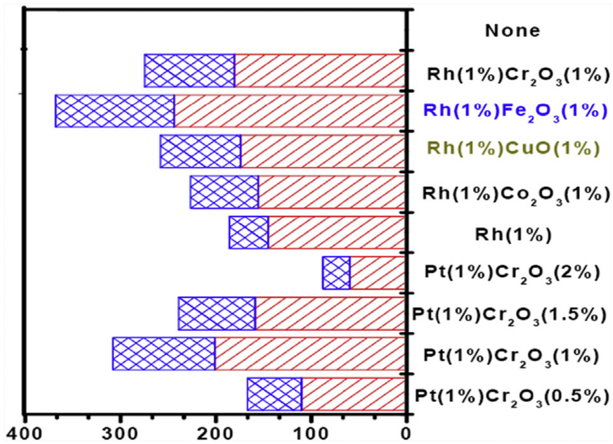

Fig. 19 – Photocatalytic activity $Bi_{0.5}Y_{0.5}VO_4$ loaded with different cocatalysts.

energy contributed by BiO_x, which cannot reduce water to H_2. By diluted acid treatment, BiO_x will be washed and the surface only formed by Y–O–V as shown in Fig. 17. The electron photo-generated will keep in the conduction band formed by BYV which can split water.

Effect of different cocatalyst

Cocatalysts loaded on the photocatalysts are considered to be indispensable for enhancing photocatalytic activity. The roles of cocatalysts in photocatalytic hydrogen generation mainly including 1) promote the separation of photogenerated carriers; 2) trap photogenerated carriers; 3) reducing the overpotential of H_2 and O_2 evolution; 4) inhibiting the backward reaction of H_2 and O_2 [101–104]. Familiar cocatalysts for H2 are noble metals or metallicity materials, such as Pt, Ni, Cdot, WC, etc. And some common cocatalysts for O_2 are metal oxides, such as AuO_x, CoO_x, RhO_x, PdO_x, IrO_x, RuO_x, etc. Sometimes, dual-cocatalysts are used in overall water splitting to promote H2 and O_2 generation simultaneously, such as Pt–Cr_2O_3, Rh–Cr_2O_3, Pt-CoO_x, etc. [105–107].

Based on the findings that photogenerated electrons and holes can be spatially separated onto the different facets of $BiVO_4$, Li et al. have successfully prepared two types of photocatalysts ($M/CoO_x/BiVO_4$ and $M/Co_3O_4/SrTiO_3$, where M stands for noble metals) with reduction and oxidation cocatalysts selectively deposited onto the {010} and {110} facets of $BiVO_4$ by a photo-deposition method, as shown in Fig. 18. Remarkably enhanced photocatalytic activities were observed

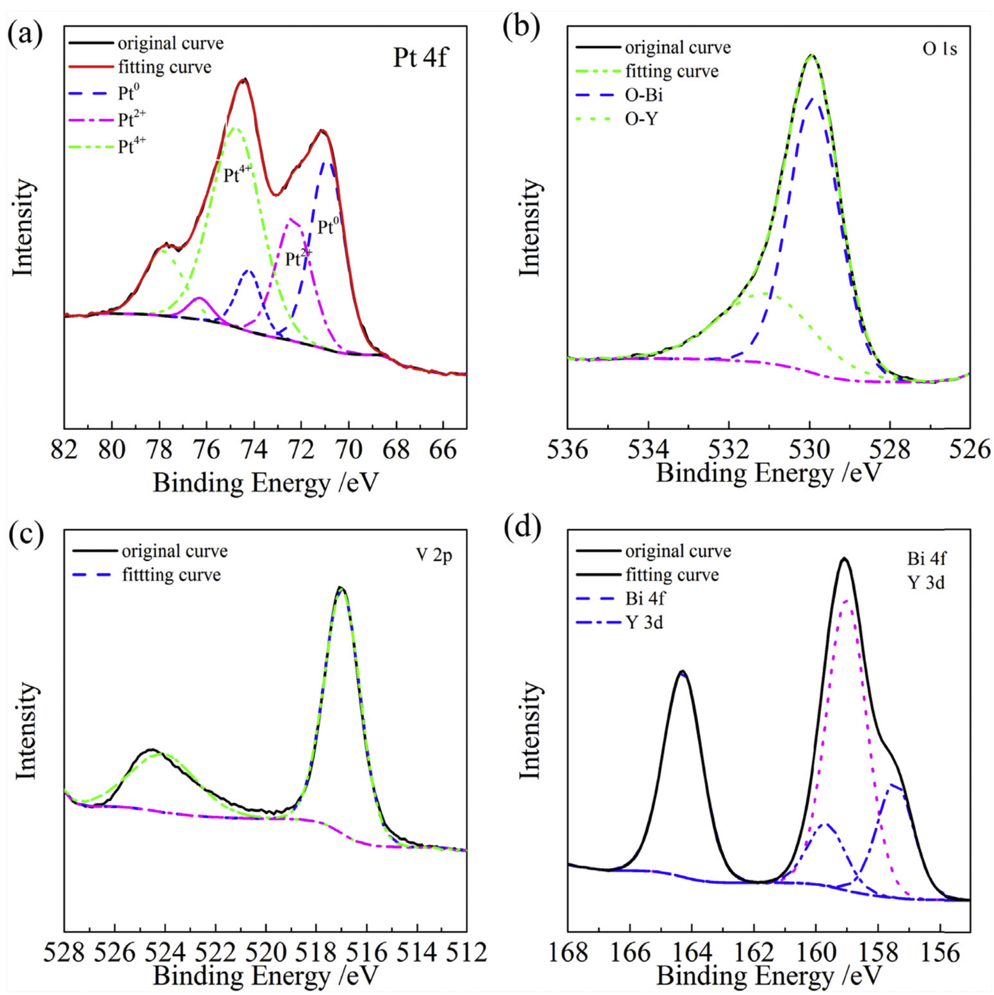

Fig. 20 – XPS analyses of Pt 4f (a), O1s (b), V2p (c) and Bi 4f, Y 3d (d) for $Bi_{0.5}Y_{0.5}VO_4$ powder samples [71].

Please cite this article as: Fang W, Shangguan W, A review on bismuth-based composite oxides for photocatalytic hydrogen generation, International Journal of Hydrogen Energy, https://doi.org/10.1016/j.ijhydene.2018.11.063

for such assembled photocatalysts in control experiments of photocatalytic activity [108,109].

Liu et al. synthesized the $BiVO_4$:YVO_4 solid solutions, and found that $Bi_{0.5}$ $Y_{0.5}VO_4$ was a stable and efficient photocatalyst for overall water splitting. The naked $Bi_{0.5}Y_{0.5}VO_4$ without cocatalysts almost could not produce H_2 or O_2, as shown in Fig. 19. $Bi_{0.5}Y_{0.5}VO_4$ with dual-cocatalysts (expecially 1 wt%Rh and 1 wt%Fe_2O_3) had a high photocatalytic activity for H_2 and O_2 evolution. Chen et al. systematically study the roles of cocatalyst in the photocatalytic reaction [110]. It is found that Pt, Rh_2O_3, NiO nanoparticles as cocatalysts loaded on $Bi_{0.5}Y_{0.5}VO_4$ solid solution photocatalysts could enhance the photocatalytic activity significantly. Among the cocatalysts in this study, Rh_2O_3 was found to give the highest photocatalytic activity. This is because, compared to Pt and NiO, Rh_2O_3 nanoparticles not only reduce more overpotential of O_2 evolution but also extremely promote the separation of electrons and holes.

Pt as cocatalyst is adverse for overall water splitting because it causes a backward reaction. By in situ photodeposition H_2PtCl_6 in pure water, it is found that $Bi_{0.5}Y_{0.5}VO_4$ can split pure water with H_2 and O_2 steadily evolve with the reaction time. It is mainly attributed to the existence of PtO_x induced by in situ photodeposition, which can suppress the undesirable hydrogen back-oxidation [111,112]. By XPS analysis of Pt(1 wt%)-$Bi_xY_{1-x}VO_4$, three pairs peaks are observed corresponding to Pt^0, Pt^{2+}, and Pt^{4+} with binding energy at 70.8, 72.4 and 74.8 eV (as shown in Fig. 20). So both metallic Pt and PtO_x coexist on the surface of Pt(1 wt%)-$Bi_xY_{1-x}VO_4$, which may also contribute to the split water with the stoichiometric ratio.

Conclusions

Bismuth-based composite oxides have a large extended family. Particularly, most of them can absorb visible-light that makes them attract much attention. However, due to their lower conduction band made up by Bi 6p and O 2p, they are failed for water splitting. In this review, we dealt with the attempts to make Bismuth-based composite oxides for photocatalytic hydrogen generation as well as the strategies for photocatalytic hydrogen generation activity improvement. Doping, quantum size effect, and solid solution are the common methods to control CBM and VBM of particle material. Especially, Bismuth-based composite oxides usually have large particle size. If their particle size can be reduced to quantum size, the CBM would shift negative to satisfy the redox potential of H^+/H_2. The $Bi_xY_{1-x}VO_4$ solid solution is an excellent photocatalyst for overall water splitting. However, the band gap of $Bi_xY_{1-x}VO_4$ is still wide which only absorb light less than 410 nm. The further study should focus on how to narrow its energy band by elevating VBM. Bismuth-based composite oxides as O2-evolution photocatalysts in the Z-scheme system is better enough compared with H2-evolution photocatalysts. The performance limitation of the Z-scheme system focuses on the H_2-evolution photocatalysts and electron mediator, which need to be solved in the future.

Acknowledgment

We thank the National Natural Science Foundation of China (21773153) and the National Key Basic Research and Development Program of China (2009CN220000) for the financial support.

REFERENCES

[1] Bard AJ, Fox MA. Artificial photosynthesis: solar splitting of water to hydrogen and oxygen. Accounts Chem Res 1994;28:141–5.
[2] Fujishima A, Honda K. Electrochemical photolysis of water at a semiconductor electrode. Nature 1972;238:37–8.
[3] Wang Q, Hisatomi T, Jia Q, Tokudome H, Zhong M, Wang C, et al. Scalable water splitting on particulate photocatalyst sheets with a solar-to-hydrogen energy conversion efficiency exceeding 1%. Nat Mater 2016;15:611–5.
[4] Wang Z, Li C, Domen K. Recent developments in heterogeneous photocatalysts for solar-driven overall water splitting. Chem Soc Rev 2018. https://doi.org/10.1039/C8CS00542G.
[5] Maeda K, Domen K. Photocatalytic water splitting: recent progress and future challenges. J Phys Chem Lett 2010;1:2655–61.
[6] Zou Z, Ye J, Sayama K, Arakawa H. Direct splitting of water under visible light irradiation with an oxide semiconductor photocatalyst. Nature 2001;414:625–7.
[7] Asahi R, Morikawa T, Ohwaki T, Aoki K, Taga Y. Visible-light photocatalysis in nitrogen-doped titanium oxides. Science 2001;293:269–71.
[8] Khan SU, Al-Shahry M, Ingler Jr WB. Efficient photochemical water splitting by a chemically modified n-TiO_2. Science 2002;297:2243–5.
[9] Umebayashi T, Yamaki T, Itoh H, Asai K. Band gap narrowing of titanium dioxide by sulfur doping. Appl Phys Lett 2002;81:454–6.
[10] Chen X, Liu L, Yu PY, Mao SS. Increasing solar absorption for photocatalysis with black hydrogenated titanium dioxide nanocrystals. Science 2011;331:746–50.
[11] Konta R, Ishii T, Kato H, Kudo A. Photocatalytic activities of noble metal ion doped $SrTiO_3$ under visible light irradiation. J Phys Chem B 2004;108:8992–5.
[12] Maeda K, Takata T, Hara M, Saito N, Inoue Y, Kobayashi H, et al. GaN:ZnO solid solution as a photocatalyst for visible-light-driven overall water splitting. J Am Chem Soc 2005;127:8286–7.
[13] Maeda K, Teramura K, Lu D, Takata T, Saito N, Inoue Y, et al. Photocatalyst releasing hydrogen from water. Nature 2006;440:295.
[14] Maeda K, Teramura K, Domen K. Effect of post-calcination on photocatalytic activity of $(Ga_{1-x}Zn_x)(N_{1-x}O_x)$ solid solution for overall water splitting under visible light. J Catal 2008;254:198–204.
[15] Wang X, Maeda K, Thomas A, Takanabe K, Xin G, Carlsson JM, et al. A metal-free polymeric photocatalyst for hydrogen production from water under visible light. Nat Mater 2009;8:76–80.
[16] Liu J, Liu Y, Liu N, Han Y, Zhang X, Huang H, et al. Metal-free efficient photocatalyst for stable visible water splitting via a two-electron pathway. Science 2015;347:970–4.
[17] Liao L, Zhang Q, Su Z, Zhao Z, Wang Y, Li Y, et al. Efficient solar water-splitting using a nanocrystalline CoO photocatalyst. Nat Nanotechnol 2014;9:69–73.

Please cite this article as: Fang W, Shangguan W, A review on bismuth-based composite oxides for photocatalytic hydrogen generation, International Journal of Hydrogen Energy, https://doi.org/10.1016/j.ijhydene.2018.11.063

[18] Tian B, Tian B, Smith B, Scott MC, Hua R, Lei Q, et al. Supported black phosphorus nanosheets as hydrogen-evolving photocatalyst achieving 5.4% energy conversion efficiency at 353 K. Nat Commun 2018;9:1397.
[19] Chowdhury FA, Trudeau ML, Guo H, Mi Z. A photochemical diode artificial photosynthesis system for unassisted high efficiency overall pure water splitting. Nat Commun 2018;9:1707.
[20] Liu MC, Chen YB, Su JZ, Shi JW, Wang XX, Guo LJ. Photocatalytic hydrogen production using twinned nanocrystals and an unanchored NiS_x co-catalyst. Nat Energy 2016;1:1–8.
[21] Yan H, Yang J, Ma G, Wu G, Zong X, Lei Z, et al. Visible-light-driven hydrogen production with extremely high quantum efficiency on Pt–PdS/CdS photocatalyst. J Catal 2009;266:165–8.
[22] Kudo A, Hijii S. H2 or O2 evolution from aqueous solutions on layered oxide photocatalysts consisting of Bi3+ with 6s2 configuration and d0 transition metal ions. Chem Lett 1999:1103–4.
[23] Tokunaga S, Kato H, Kudo A. Selective preparation of monoclinic and tetragonal $BiVO_4$ with scheelite structure and their photocatalytic properties. Chem Mater 2001;13:4624–8.
[24] Zhao H, Tian F, Wang R, Chen R. A review on bismuth-related nanomaterials for photocatalysis. Reviews in Advanced Sciences and Engineering 2014;3:3–27.
[25] M A, M J, Ashokkumar M, Arunachalam P. A review on $BiVO_4$ photocatalyst: activity enhancement methods for solar photocatalytic applications. Appl Catal Gen 2018;555:47–74.
[26] Zhang L, Zhu Y. A review of controllable synthesis and enhancement of performances of bismuth tungstate visible-light-driven photocatalysts. Catalysis Science & Technology 2012;2:694–706.
[27] Martinez Suarez C, Hernández S, Russo N. $BiVO_4$ as photocatalyst for solar fuels production through water splitting: a short review. Appl Catal Gen 2015;504:158–70.
[28] Meng X, Zhang Z. Bismuth-based photocatalytic semiconductors: Introduction, challenges and possible approaches. J Mol Catal Chem 2016;423:533–49.
[29] Ye L, Su Y, Jin X, Xie H, Zhang C. Recent advances in BiOX (X = Cl, Br and I) photocatalysts: synthesis, modification, facet effects and mechanisms. Environmental Science-Nano. 2014;1:90–112.
[30] Park Y, McDonald KJ, Choi KS. Progress in bismuth vanadate photoanodes for use in solar water oxidation. Chem Soc Rev 2013;42:2321–37.
[31] Liu C, Li X, Su J, Guo L. Enhanced charge separation in copper incorporated $BiVO_4$ with gradient doping concentration profile for photoelectrochemical water splitting. Int J Hydrogen Energy 2016;41:12842–51.
[32] Ma D, Wu J, Gao M, Xin Y, Ma T, Sun Y. Fabrication of Z-scheme $g\text{-}C_3N_4$/RGO/Bi_2WO_6 photocatalyst with enhanced visible-light photocatalytic activity. Chem Eng J 2016;290:136–46.
[33] Zhao Y, Fan H, Fu K, Ma L, Li M, Fang J. Intrinsic electric field assisted polymeric graphitic carbon nitride coupled with $Bi_4Ti_3O_{12}/Bi_2Ti_2O_7$ heterostructure nanofibers toward enhanced photocatalytic hydrogen evolution. Int J Hydrogen Energy 2016;41:16913–26.
[34] Lakshmana Reddy N, Emin S, Valant M, Shankar MV. Nanostructured Bi_2O_3@TiO_2 photocatalyst for enhanced hydrogen production. Int J Hydrogen Energy 2017;42:6627–36.
[35] Chang C-J, Wang C-W, Wei Y-H, Chen C-Y. Enhanced photocatalytic H_2 production activity of Ag-doped Bi_2WO_6-graphene based photocatalysts. Int J Hydrogen Energy 2018;43:11345–54.
[36] He R, Xu D, Cheng B, Yu J, Ho W. Review on nanoscale Bi-based photocatalysts. Nanoscale Horizons 2018;3:464–504.
[37] Walsh A, Watson GW, Payne DJ, Edgell RG, Guo J, Glans P-A, et al. Electronic structure of theαandδphases of Bi_2O_3: a combined ab initio and X-ray spectroscopy study. Phys Rev B 2006;73:235104.
[38] Zhang L, Xu T, Zhao X, Zhu Y. Controllable synthesis of Bi_2MoO_6 and effect of morphology and variation in local structure on photocatalytic activities. Appl Catal B Environ 2010;98:138–46.
[39] Tian G, Chen Y, Zhou W, Pan K, Dong Y, Tian C, et al. Facile solvothermal synthesis of hierarchical flower-like Bi_2MoO_6 hollow spheres as high performance visible-light driven photocatalysts. J Mater Chem 2011;21:887–92.
[40] Liu H, Yuan J, Shangguan W, Teraoka Y. Visible-Light-Responding $BiYWO_6$ solid solution for stoichiometric photocatalytic water splitting. J Phys Chem C 2008;112:8521–3.
[41] Fu H, Zhang L, Yao W, Zhu Y. Photocatalytic properties of nanosized Bi_2WO_6 catalysts synthesized via a hydrothermal process. Appl Catal B Environ 2006;66:100–10.
[42] Tang J, Zou Z, Ye J. Photocatalytic decomposition of organic contaminants by Bi2WO6Under visible light irradiation. Catal Lett 2004;92:53–6.
[43] Wang BC, Nisar J, Pathak B, Kang TW, Ahuja R. Band gap engineering in $BiNbO_4$ for visible-light photocatalysis. Appl Phys Lett 2012;100:6804–38.
[44] Zhai H-F, Li A-D, Kong J-Z, Li X-F, Zhao J, Guo B-L, et al. Preparation and visible-light photocatalytic properties of $BiNbO_4$ and $BiTaO_4$ by a citrate method. J Solid State Chem 2013;202:6–14.
[45] Lv Y, Zhu Y, Zhu Y. Enhanced photocatalytic performance for the $BiPO_{4-x}$ nanorod induced by surface oxygen vacancy. J Phys Chem C 2013;117:18520–8.
[46] Yang Y, Zhang C, Lai C, Zeng G, Huang D, Cheng M, et al. BiOX (X=Cl, Br, I) photocatalytic nanomaterials: applications for fuels and environmental management. Adv Colloid Interface Sci 2018;254:76–93.
[47] Luo J, Maggard PA. Hydrothermal synthesis and photocatalytic activities of $SrTiO_3$-coated Fe_2O_3 and $BiFeO_3$. Adv Mater 2006;18:514–7.
[48] Qin Z-z, Liu Z-l, Liu Y-b, Yang K-d. Synthesis of $BiYO_3$ for degradation of organic compounds under visible-light irradiation. Catal Commun 2009;10:1604–8.
[49] Madhusudan P, Ran J, Zhang J, Yu J, Liu G. Novel urea assisted hydrothermal synthesis of hierarchical $BiVO_4/Bi_2O_2CO_3$ nanocomposites with enhanced visible-light photocatalytic activity. Appl Catal B Environ 2011;110:286–95.
[50] Zheng H, Zhang T, Zhu Y, Liang B, Jiang W. $KBiO_3$ as an effective visible-light-driven photocatalyst: degradation mechanism for different organic pollutants. ChemPhotoChem 2018;2:442–9.
[51] Takei T, Haramoto R, Dong Q, Kumada N, Yonesaki Y, Kinomura N, et al. Photocatalytic activities of various pentavalent bismuthates under visible light irradiation. J Solid State Chem 2011;184:2017–22.
[52] Xu N, Li F, Gao L, Hu H, Hu Y, Long X, et al. Polythiophene coated $CuBi_2O_4$ networks: a porous inorganic–organic hybrid heterostructure for enhanced photoelectrochemical hydrogen evolution. Int J Hydrogen Energy 2018;43:2064–72.
[53] Murugesan S, Subramanian VR. Robust synthesis of bismuth titanate pyrochlore nanorods and their photocatalytic applications. Chem commun 2009:5109–11.
[54] Wang L, Wang W, Shang M, Sun S, Yin W, Ren J, et al. Visible light responsive bismuth niobate photocatalyst: enhanced contaminant degradation and hydrogen generation. J Mater Chem 2010;20:8405.

Please cite this article as: Fang W, Shangguan W, A review on bismuth-based composite oxides for photocatalytic hydrogen generation, International Journal of Hydrogen Energy, https://doi.org/10.1016/j.ijhydene.2018.11.063

[55] Yang J, Jiang P, Yue M, Yang D, Cong R, Gao W, et al. $Bi_2Ga_4O_9$: an undoped single-phase photocatalyst for overall water splitting under visible light. J Catal 2017;345:236–44.
[56] Wang L, Wang W. Photocatalytic hydrogen production from aqueous solutions over novel $Bi_{0.5}Na_{0.5}TiO_3$ microspheres. Int J Hydrogen Energy 2012;37:3041–7.
[57] Li Z, Wang Y, Liu J, Chen G, Li Y, Zhou C. Photocatalytic hydrogen production from aqueous methanol solutions under visible light over $Na(Bi_xTa_{1-x})O_3$ solid-solution. Int J Hydrogen Energy 2009;34:147–52.
[58] Kanhere P, Zheng J, Chen Z. Visible light driven photocatalytic hydrogen evolution and photophysical properties of Bi^{3+} doped $NaTaO_3$. Int J Hydrogen Energy 2012;37:4889–96.
[59] Lee G-J, Zheng Y-C, Wu JJ. Fabrication of hierarchical bismuth oxyhalides (BiOX, X = Cl, Br, I) materials and application of photocatalytic hydrogen production from water splitting. Catal Today 2018;307:197–204.
[60] Fujito H, Kunioku H, Kato D, Suzuki H, Higashi M, Kageyama H, et al. Layered perovskite oxychloride Bi_4NbO_8Cl: a stable visible light responsive photocatalyst for water splitting. J Am Chem Soc 2016;138:2082–5.
[61] Wei Z, Liu J, Fang W, Qin Z, Jiang Z, Shangguan W. Enhanced photocatalytic hydrogen evolution using a novel in situ heterojunction yttrium-doped $Bi_4NbO_8Cl@Nb_2O_5$. Int J Hydrogen Energy 2018;43:14281–92.
[62] Sharma G, Zhao Z, Sarker P, Nail BA, Wang J, Huda MN, et al. Electronic structure, photovoltage, and photocatalytic hydrogen evolution with p-$CuBi_2O_4$ nanocrystals. J Mater Chem 2016;4:2936–42.
[63] Lu L, Lv M, Wang D, Liu G, Xu X. Efficient photocatalytic hydrogen production over solid solutions $Sr_{1-x}BixTi_{1-x}FexO_3$ ($0\leq x \leq0.5$). Appl Catal B Environ 2017;200:412–9.
[64] Hou J, Cao R, Wang Z, Jiao S, Zhu H. Chromium-doped bismuth titanate nanosheets as enhanced visible-light photocatalysts with a high percentage of reactive {110} facets. J Mater Chem 2011;21:7296–301.
[65] Chen Z, Jiang X, Zhu C, Shi C. Chromium-modified $Bi_4Ti_3O_{12}$ photocatalyst: application for hydrogen evolution and pollutant degradation. Appl Catal B Environ 2016;199:241–51.
[66] Almeida CG, Araujo RB, Yoshimura RG, Mascarenhas AJS, Ferreira da Silva A, Araujo CM, et al. Photocatalytic hydrogen production with visible light over Mo and Cr-doped $BiNb(Ta)O_4$. Int J Hydrogen Energy 2014;39:1220–7.
[67] Nagabhushana GP, Nagaraju G, Chandrappa GT. Synthesis of bismuth vanadate: its application in H2evolution and sunlight-driven photodegradation. J Mater Chem 2013;1:388–94.
[68] Sun S, Wang W, Li D, Zhang L, Jiang D. Solar light driven pure water splitting on quantum sized $BiVO_4$ without any cocatalyst. ACS Catal 2014;4:3498–503.
[69] Pan B, Wang Y, Liang Y, Luo S, Su W, Wang X. Nanocomposite of $BiPO_4$ and reduced graphene oxide as an efficient photocatalyst for hydrogen evolution. Int J Hydrogen Energy 2014;39:13527–33.
[70] Sun Z, Guo J, Zhu S, Mao L, Ma J, Zhang D. A high-performance Bi_2WO_6-graphene photocatalyst for visible light-induced H_2 and O_2 generation. Nanoscale 2014;6:2186–93.
[71] Wang Q, Liu H, Jiang L, Yuan J, Shangguan W. Visible-light-responding $Bi_{0.5}Dy_{0.5}VO_4$ solid solution for photocatalytic water splitting. Catal Lett 2009;131:160–3.
[72] Wang Q, An N, Mu R, Liu H, Yuan J, Shi J, et al. Photocatalytic water splitting by band-gap engineering of solid solution $Bi_{1-x}Dy_xVO_4$ and $Bi_{0.5}M_{0.5}VO_4$ (M=La, Sm, Nd, Gd, Eu, Y). J Alloy Comp 2012;522:19–24.
[73] Liu H, Yuan J, Jiang Z, Shangguan W, Einaga H, Teraoka Y. Novel photocatalyst of V-based solid solutions for overall water splitting. J Mater Chem 2011;21:16535–43.
[74] Liu H, Yuan J, Jiang Z, Shangguan W, Einaga H, Teraoka Y. Roles of Bi, M and VO_4 tetrahedron in photocatalytic properties of novel $Bi_{0.5}M_{0.5}VO_4$ (M=La, Eu, Sm and Y) solid solutions for overall water splitting. J Solid State Chem 2012;186:70–5.
[75] Fang W, Jiang Z, Yu L, Liu H, Shangguan W, Terashima C, et al. Novel dodecahedron $BiVO_4$:YVO_4 solid solution with enhanced charge separation on adjacent exposed facets for highly efficient overall water splitting. J Catal 2017;352:155–9.
[76] Fang W, Liu J, Yang D, Wei Z, Jiang Z, Shangguan W. Effect of surface self-heterojunction existed in $Bi_xY_{1-x}VO_4$ on photocatalytic overall water splitting. ACS Sustainable Chem Eng 2017;5:6578–84.
[77] Yu L, Fang W, Liu J, Qin Z, Jiang Z, Shangguan W. $Bi_xY_{1-x}VO_4$ solid solution with porous surface synthesized by molten salt method for photocatalytic water splitting. Int J Hydrogen Energy 2017;42:6519–25.
[78] Wang Q, An N, Chen W, Wang R, Wang F, Lei Z, et al. Photocatalytic water splitting into hydrogen and research on synergistic of Bi/Sm with solid solution of Bi–Sm–V photocatalyst. Int J Hydrogen Energy 2012;37:12886–92.
[79] Kim TW, Ping Y, Galli GA, Choi KS. Simultaneous enhancements in photon absorption and charge transport of bismuth vanadate photoanodes for solar water splitting. Nat Commun 2015;6:8769.
[80] Kato H, Hori M, Konta R, Shimodaira Y, Kudo A. Construction of Z-scheme type heterogeneous photocatalysis systems for water splitting into H_2 and O_2 under visible light irradiation. Chem Lett 2004;33:1348–9.
[81] Sasaki Y, Iwase A, Kato H, Kudo A. The effect of co-catalyst for Z-scheme photocatalysis systems with an Fe^{3+}/Fe^{2+} electron mediator on overall water splitting under visible light irradiation. J Catal 2008;259:133–7.
[82] Sasaki Y, Nemoto H, Saito K, Kudo A. Solar water splitting using powdered photocatalysts driven by Z-Schematic interparticle electron transfer without an electron mediator. J Phys Chem C 2009;113:17536–42.
[83] Jia Q, Iwase A, Kudo A. $BiVO_4$–Ru/$SrTiO_3$:Rh composite Z-scheme photocatalyst for solar water splitting. Chem Sci 2014;5:1513–9.
[84] Iwase A, Ng YH, Ishiguro Y, Kudo A, Amal R. Reduced graphene oxide as a solid-state electron mediator in Z-scheme photocatalytic water splitting under visible light. J Am Chem Soc 2011;133:11054–7.
[85] Wu X, Zhao J, Wang L, Han M, Zhang M, Wang H, et al. Carbon dots as solid-state electron mediator for $BiVO_4$/CDs/CdS Z-scheme photocatalyst working under visible light. Appl Catal B Environ 2017;206:501–9.
[86] Pan Z, Hisatomi T, Wang Q, Chen S, Nakabayashi M, Shibata N, et al. Photocatalyst sheets composed of particulate $LaMg_{1/3}Ta_{2/3}O_2N$ and Mo-doped $BiVO_4$ for Z-Scheme water splitting under visible light. ACS Catal 2016;6:7188–96.
[87] Wang Q, Hisatomi T, Suzuki Y, Pan Z, Seo J, Katayama M, et al. Particulate photocatalyst sheets based on carbon conductor layer for efficient Z-Scheme pure-water splitting at ambient pressure. J Am Chem Soc 2017;139:1675–83.
[88] Qin Z, Fang W, Liu J, Wei Z, Jiang Z, Shangguan W. Zinc-doped g-C_3N_4/$BiVO_4$ as a Z-scheme photocatalyst system for water splitting under visible light. Chin J Catal 2018;39:472–8.
[89] Yang HG, Sun CH, Qiao SZ, Zou J, Liu G, Smith SC, et al. Anatase TiO_2 single crystals with a large percentage of reactive facets. Nature 2008;453:638–41.

Please cite this article as: Fang W, Shangguan W, A review on bismuth-based composite oxides for photocatalytic hydrogen generation, International Journal of Hydrogen Energy, https://doi.org/10.1016/j.ijhydene.2018.11.063

[90] Ohno T, Sarukawa K, Matsumura M. Crystal faces of rutile and anatase TiO_2 particles and their roles in photocatalytic reactions. New J Chem 2002;26:1167–70.
[91] Pan J, Liu G, Lu GQ, Cheng HM. On the true photoreactivity order of {001}, {010}, and {101} facets of anatase TiO_2 crystals. Angew Chem Int Ed 2011;50:2133–7.
[92] Gordon TR, Cargnello M, Paik T, Mangolini F, Weber RT, Fornasiero P, et al. Nonaqueous synthesis of TiO_2 nanocrystals using TiF_4 to engineer morphology, oxygen vacancy concentration, and photocatalytic activity. J Am Chem Soc 2012;134:6751–61.
[93] Li R, Zhang F, Wang D, Yang J, Li M, Zhu J, et al. Spatial separation of photogenerated electrons and holes among {010} and {110} crystal facets of $BiVO_4$. Nat Commun 2013;4:1432.
[94] Tachikawa T, Ochi T, Kobori Y. Crystal-Face-Dependent charge dynamics on a $BiVO_4$ photocatalyst revealed by single-particle spectroelectrochemistry. ACS Catal 2016;6:2250–6.
[95] Li P, Chen X, He H, Zhou X, Zhou Y, Zou Z. Polyhedral 30-faceted $BiVO_4$ microcrystals predominantly enclosed by high-index planes promoting photocatalytic water-splitting activity. Adv Mater 2018;30:170319.
[96] Huang Y, Li H, Balogun MS, Liu W, Tong Y, Lu X, et al. Oxygen vacancy induced bismuth oxyiodide with remarkably increased visible-light absorption and superior photocatalytic performance. ACS Appl Mater Interfaces 2014;6:22920–7.
[97] Li J, Wu X, Pan W, Zhang G, Chen H. Vacancy-rich monolayer BiO_{2-x} as a highly efficient UV, visible, and near-infrared responsive photocatalyst. Angew Chem Int Ed 2017;57:491–5.
[98] Ding K, Chen B, Fang Z, Zhang Y, Chen Z. Why the photocatalytic activity of Mo-doped $BiVO_4$ is enhanced: a comprehensive density functional study. Phys Chem Chem Phys 2014;16:13465–76.
[99] Zhang Y, Guo Y, Duan H, Li H, Sun C, Liu H. Facile synthesis of V(4+) self-doped, [010] oriented $BiVO_4$ nanorods with highly efficient visible light-induced photocatalytic activity. Phys Chem Chem Phys 2014;16:24519–26.
[100] Rossell MD, Agrawal P, Borgschulte A, Hébert C, Passerone D, Erni R. Direct evidence of surface reduction in monoclinic $BiVO_4$. Chem Mater 2015;27:3593–600.
[101] Ran J, Zhang J, Yu J, Jaroniec M, Qiao SZ. Earth-abundant cocatalysts for semiconductor-based photocatalytic water splitting. Chem Soc Rev 2014;43:7787–812.
[102] Chen X, Chen W, Lin P, Yang Y, Gao H, Yuan J, et al. In situ photodeposition of nickel oxides on CdS for highly efficient hydrogen production via visible-light-driven photocatalysis. Catal Commun 2013;36:104–8.
[103] Gao H, Chen W, Yuan J, Jiang Z, Hu G, Shangguan W, et al. Controllable O2•− oxidization graphene in TiO_2/graphene composite and its effect on photocatalytic hydrogen evolution. Int J Hydrogen Energy 2013;38:13110–6.
[104] Chen XP, Chen W, Gao HY, Yang Y, Shangguan WF. In situ photodeposition of NiO_x on CdS for hydrogen production under visible light: enhanced activity by controlling solution environment. Appl Catal B Environ 2014;152:68–72.
[105] Meng A, Zhang J, Xu D, Cheng B, Yu J. Enhanced photocatalytic H_2 production activity of anatase TiO_2 nanosheet by selectively depositing dual-cocatalysts on {101} and {001} facets. Appl Catal B Environ 2016;198:286–94.
[106] Liu M, You W, Lei Z, Zhou G, Yang J, Wu G, et al. Water reduction and oxidation on Pt-Ru/$Y_2Ta_2O_5N_2$ catalyst under visible light irradiation. Chem commun 2004:2192–3.
[107] Maeda K, Teramura K, Lu D, Takata T, Saito N, Inoue Y, et al. Characterization of Rh-Cr mixed-oxide nanoparticles dispersed on $(Ga_{(1-x)}Zn_{(x)})(N_{(1-x)}O_x)$ as a cocatalyst for visible-light-driven overall water splitting. J Phys Chem B 2006;110:13753–8.
[108] Li R, Han H, Zhang F, Wang D, Li C. Highly efficient photocatalysts constructed by rational assembly of dual-cocatalysts separately on different facets of $BiVO_4$. Energy Environ Sci 2014;7:1369–76.
[109] Mu L, Zhao Y, Li A, Wang S, Wang Z, Yang J, et al. Enhancing charge separation on high symmetry $SrTiO_3$ exposed with anisotropic facets for photocatalytic water splitting. Energy Environ Sci 2016;9:2463–9.
[110] Chen W, Yang B, Yu Q, Mao L, Fan Z, Wang Q, et al. Effect of Rh oxide as a cocatalyst over $Bi_{0.5}Y_{0.5}VO_4$ on photocatalytic overall water splitting. Appl Surf Sci 2015;355:1069–74.
[111] Zhang GG, Lan ZA, Lin LH, Lin S, Wang XC. Overall water splitting by Pt/g-C_3N_4 photocatalysts without using sacrificial agents. Chem Sci 2016;7:3062–6.
[112] Li YH, Xing J, Chen ZJ, Li Z, Tian F, Zheng LR, et al. Unidirectional suppression of hydrogen oxidation on oxidized platinum clusters. Nat Commun 2013;4:2500.

Please cite this article as: Fang W, Shangguan W, A review on bismuth-based composite oxides for photocatalytic hydrogen generation, International Journal of Hydrogen Energy, https://doi.org/10.1016/j.ijhydene.2018.11.063